STRUCTURAL INTERPRETATION OF GRAPHITE-BEARING BLACK SCHIST IN AITOLAMPI, EASTERN FINLAND

Sammanfattning:

STRUKTURGEOLOGISK TOLKNING AV GRAFITBÄRANDE SVARTSKIFFER I AITOLAMPI, ÖSTRA FINLAND

Master's thesis
Geology and mineralogy
Faculty of Science and Engineering
Åbo Akademi University, spring 2018
Laura Puronaho, 37615

PURONAHO LAURA, 2018: *Structural interpretation of graphite-bearing black schist in Aitolampi area, Eastern Finland*. Swedish Summary - Svensk sammanfattning: Strukturgeologisk tolkning av grafitbärande svartskiffer i Aitolampi, Östra Finland. 64 p., 32 figures, 4 appendices. Åbo Akademi University. Faculty of Science and Engineering, Geology and Mineralogy, spring 2018.

This master's thesis is a part of the *FennoFlakes*-project with Åbo Akademi University and Geological Survey of Finland. The studies in this thesis are conducted within the exploration section in association with Beowulf Mining plc.

Keywords: Graphite, black schist, structural geology, shear zones, eastern Finland

ABSTRACT

Graphite is a mineral consisting of layers of carbon stacked on top of each other. One layer of carbon is called graphene and forms a two-dimensional lattice. Naturally occurring graphite belongs to the European Union's top 30 most critical minerals and has a high import reliance rate. Graphite's economic value and demand is increasing and it has exceptional features within high –tech applications due to its excellent features in conductance of heat and electricity. During the years 1760-1947, 30 flake graphite deposits have been exploited in Finland. According to the Geological Survey of Finland, Finland has a good potential for new flake graphite deposits due to the qualities of the bedrock and a suitable metamorphic grade.

The aim of this study was to interpret the structural setting in Aitolampi area. Data from electromagnetic measurements, stereographic projections, mapping data from drill cores and published studies from the area were utilized. Aitolampi (from Lake Aitolampi) is located in the town called Heinävesi, in southern Savonia, eastern Finland. This particular area was chosen because graphite occurrences have been known in the nearby Haapamäki area since the late 19th century. The electromagnetic measurements and geological mapping and sampling have given positive results regarding the presence of graphite in the bedrock.

Interpretations of the stereographic projections points to a large-scale double-plunging antiformal structure, with fold axes in both northwest and southeast. Based on the structural measurements from drill cores, 2D cross sections of the structural setting were constructed. The folds present in Aitolampi are isoclinal and the axial planes are inclined towards southwest. When the cross cuts are combined with Slingram measurements, it appears that the folds have an undulating hinge-line and the graphite enrichment seems to be located in the antiforms and in the parasitic folds located in the fold limbs. Aitolampi is interpreted to be located between two deformation zones and thrusted upwards from its surroundings, due to the compressional stress.

TABLE OF CONTENTS

APPENDICES

1. INTRODUCTION

The aim of this study is to understand the structural setting in the Aitolampi study area by using structural measurements, drill core data and electromagnetic measurements.

Graphite is a mineral consisting of layers of pure carbon. The layers consist of graphene which is composed of carbon atoms bonded to each other in a hexagonal two-dimensional structure. Graphite exists as crystalline-, amorphous- and vein-type. It is an excellent conductor of heat and electricity and has several chemical, physical and nuclear (nuclear-fission applications) properties for high-tech applications (Pierson 1993).

Graphite has been ranked to the top 30 critical minerals in 2017 by the European Union (EU 2017). The list is based on risks of supply shortage and a higher economic impact than other raw materials. The Import Reliance Rate (IRR) of graphite to EU is 99%. This takes into account global supply and actual EU sourcing of the mineral (EC 2017). Since 2005 the price of graphite has tripled and the demand is increasing rapidly (Simandl *et al.* 2015). In the year 2004 the global natural graphite production was estimated to approximately 1.17 million tons, most of it originating from China (67%). Main exporters of graphite into EU (2010-2014) were China (63%), Brazil (17%) and Norway (7%)(EC 2017). Most of the graphite produced is used in electrodes, lubricants, batteries and refractories. Graphite is a critical material in industrialized countries and has a market with a fast forecasted growth. Lithium-ion batteries, large-scale energy storing and graphite derivates are only a few examples of high-tech use of graphite (Simandl *et al.* 2015).

According to Geological Survey of Finland (GTK), the potential for new flake graphite discoveries in Finland is good due to the qualities of the bedrock and the suitable metamorphic grade. The airborne electromagnetic measurements that cover most of Finland make the localization of deposits easier since graphite is a great conductor of electricity (Ahtola & Kuusela 2015).

The Aitolampi (from Lake Aitolampi) study area is located in Heinävesi, Eastern Finland (Figure 1). The study area is a part of the larger Haapamäki area that was

chosen due to the known occurrences of graphite. The rocks in the study area are a part of the Karelian domain consisting of Paleoproterozoic supracrustal rocks. The bedrock in the area is mainly composed of paragneiss, originally consisting of sands and clays deposited at the sea bottom. The Aitolampi area could be a continuation to the graphite-bearing Haapamäki fold, but the Kallavesi-Suvasvesi deformation zone (KSdz) is located between the areas and cutting the structures. Small-scale mining has taken place mainly in three locations in the Haapamäki area in the late 19th century (Ahtola & Kuusela 2015). The airborne electromagnetic studies, Slingram-measurements and geological mapping and sampling have given positive results when it comes to the presence of graphite deposits in Aitolampi.

This thesis is a part of the *FennoFlakes*-project, which involves Åbo Akademi University (ÅAU), the Geological Survey of Finland (GTK) and Beowulf Mining plc. Based on the structural setting, an eventual correlation between graphite-grade and specific structural setting is recognized in this thesis.

In this thesis the term 'graphite schist' rather than graphite-bearing black schist is used when the amount of graphite present in the bedrock is or exceeds 3%. This distinguishes the presence of graphite in the bedrock even in lower amounts.

Figure 1. Aitolampi (black dot) is located in eastern Finland, approximately 50 kilometers SW of Outokumpu. (Modified after National Land Survey of Finland 2013)

2. GRAPHITE

2.1 Properties of graphite

Carbon is a common chemical element with the symbol C and the atomic number 6. It is the fourth most abundant element in the universe by its mass after hydrogen, helium and oxygen. Carbon forms different allotropes when the atoms are bonded in different ways. Graphite and diamond are both different allotropes of carbon with different physical properties, graphite being one of the softest substances and diamond being the hardest naturally occurring substance. Carbon may form organic, inorganic and organometallic compounds. Carbon is capable of forming compounds with at least 80 different elements, including carbon itself (Pierson 1993; Asbury 2016).

Each carbon atom in graphite is covalently bonded to three other carbon atoms and forms a hexagonal crystal lattice (Figure 2) or a rare rhombohedral structure. These networks form two-dimensional sheets with the thickness of one atom and are called graphene layers. The sheets are connected with weak van der Waals-bonds and results in low hardness, slippery feel and perfect cleavage. It has a density of 2,26 g/cm^3. Graphite contains delocalized electrons which gives it the excellent electrical conductivity (Pierson 1993; Asbury 2016).

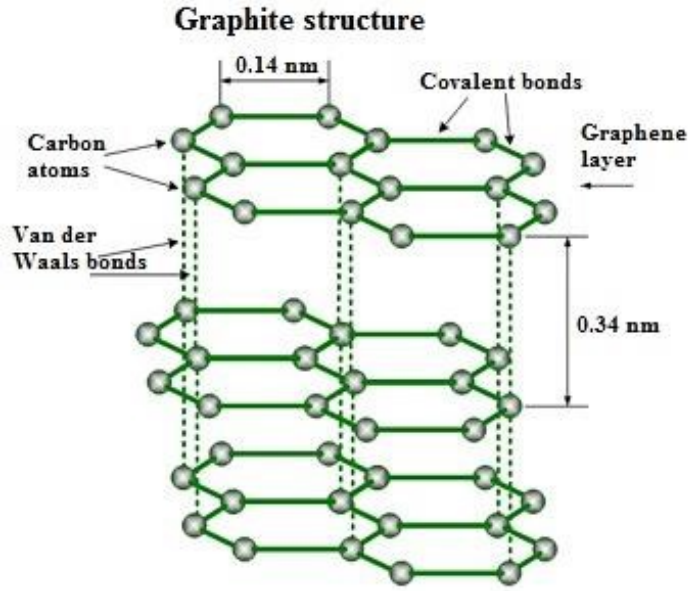

Figure 2. The crystal lattice of hexagonal graphite. Weak Van der Waals- bonds are located between the graphene layers and covalent bonds within the hexagonal structures. (Modified after Kopeliovich 2012)

Graphite can be found in metamorphic and igneous rocks. Minerals that occur with the graphite-rich rock types are quartz, plagioclase, feldspar, biotite, muscovite, pyrite and magnetite (Asbury 2016). The graphite-bearing rocks are usually schistose and have a clearly visible foliation. The grain size is most often fine and the texture is granoblastic. The mineral graphite is usually silver-grey or black depending on the grain/ flake size and type (Asbury 2016).

During the metamorphosis and diagenesis, the reduction of the kerogenic material begins and the material loses hydrocarbons, oxygen and hydrogen. The carbon is more or less amorphous during the zeolite-facies metamorphosis (~200˚C and 2 kbar). During the greenschist facies (~450˚C and 5 kbar), carbon becomes partly ordered and the crystalline graphite is present in albite-epidote-amphibolite facies (~550˚C and 7 kbar) and in the amphibolite-facies rocks (~600˚C and 8 kbar) (Landis 1971). The temperature has a great impact when it comes to the formation of graphite; the temperature has to exceed 400˚C in order to form crystalline graphite. The degree of crystallinity (how well it is ordered) depends also on the degree of metamorphosis (Simandl *et al.* 2015, Kukkonen 1984). Most of the Finnish bedrock has metamorphosed to at least the greenschist facies and therefore the carbon is to a certain extent present as graphite in the bedrock (e.g. Hölttä & Heilimo 2017).

Due to the good galvanic features in graphite, it serves as a good conductor even in relatively low amounts. Electromagnetic measurements (e.g. Slingram) are a way to reveal and localize undiscovered graphite deposits. Graphite or graphite-bearing rocks are seldom present as outcrops due to their softness and low weathering-resistance. Therefore, the electromagnetic measurements are of great importance when it comes to exploration of graphite (Kukkonen 1984; Loukola-Ruskeeniemi *et al.* 2011).

2.2 The graphite-bearing black schist

Black schist consist of silica (Si), aluminum (Al), iron (Fe), magnesium (Mg), calcium (Ca), potassium (K), >1% organic carbon (C), >1% sulphides (S), trace elements and heavy metals (e.g. Äikäs 2012). Black schists are formed in anaerobic conditions when

organic material is reduced in sea bottoms and later subjected to metamorphosis (Loukola-Ruskeeniemi 1992). There are different definitions on graphite- and black schist. Loukola-Ruskeeniemi (1992) defines mica schists containing 0.1-1% graphitic carbon as graphite-bearing mica schists, whereas over 1% of graphitic carbon occurring with more than 1% sulphur to be called black schists.

The anomalies interpreted from the airborne data in black schists are caused by the presence of graphite and/ or sulphides in the schist (Figure 3). The petrophysical properties of black schist vary based on the mineral composition (especially graphite and sulphides) and the structure of the black schist unit (Loukola-Ruskeeniemi *et al.* 2011).

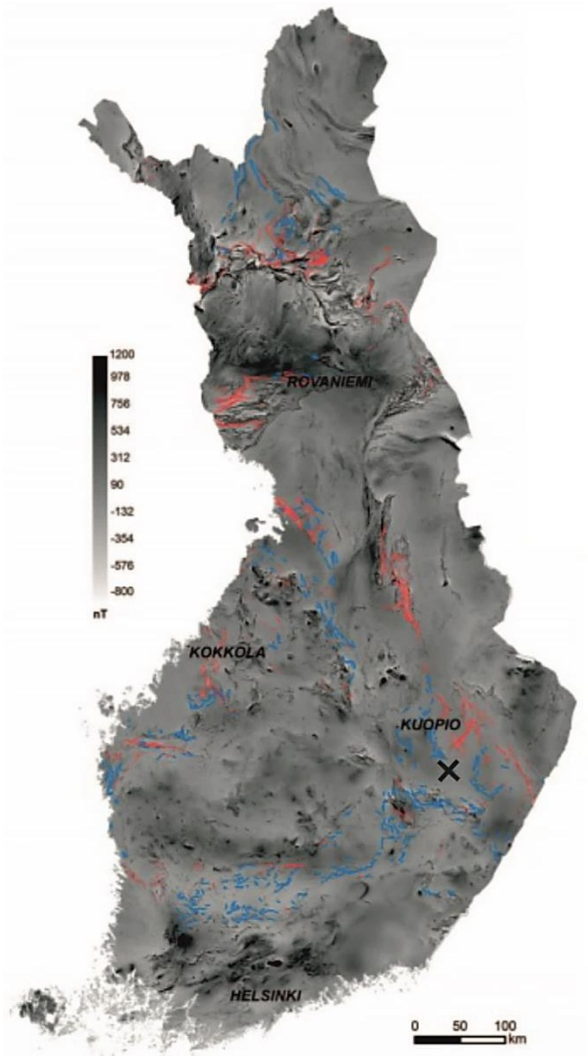

Figure 3. The black shale units in a total intensity magnetic map, conducted with low-altitude airborne measurements. Red areas are black shale verified by drill cores and in outcrops. The blue areas represent the potential areas for black shale units, also interpreted from low-altitude airborne electromagnetic data. Aitolampi marked with a black cross. (Loukola-Ruskeeniemi et al. 2011)

2.3 Types and formation of graphite

There are three main types of naturally occurring graphite; amorphous, vein-type (crystalline) and flake graphite (Simandl *et al.* 2015).

Amorphous graphite is used as a lubricant due to the small crystal-size in products requiring low reflectance. It is regarded as the cheapest form of graphite, but is still chemically stable, conductive and lubricious. Most of these microcrystalline graphite deposits are formed by contact metamorphosis from a sub-greenschist to greenschist facies or by regional metamorphosis of coal seams. These types of deposits consist of small graphite particles that are intergrown with impurities and resemble lens-shaped beds that have been affected by deformation and repeated folding and faulting. The deposits may consist of several meter thick beds and can be exposed for several hundreds of meters along strike. These deposits contain in general more than 80% graphite (30-95%) (Simandl *et al.* 2015).

The **vein type** or the crystalline graphite deposits are the most significant when it comes to economic aspects, due to its rarity and an exceptionally high quality. The vein type of graphite is found in metasedimentary belts metamorphosed to upper amphibolite or granulite facies. In these belts the deposits are found in skarn-type assemblages near to igneous intrusions, in the intrusions or in zones with a retrograde overprint (Simandl *et al.* 2015). Vein type of graphite can also be encountered in shear zones (e.g. Oohashi 2011).

Flake graphite is found disseminated in paragneisses, Si-rich quartzites and marbles that have been subjected to metamorphosis in upper amphibolite or granulite facies (Pierson 1993). It has the highest economic value of graphite types. An even mineralization of graphite with a general grade of approximately 3% is common in deposits consisting of thick sequences of paragneiss (Simandl *et al.* 2015). In some deposits (e.g. Troms, Norway), highest grades of graphite has been encountered in fold hinge zones (Henderson & Kendrick 2003). Epidote and chlorite are examples of retrograde minerals that have occasionally been encountered in high-grade graphite areas. The crystalline flake deposits are usually targeted in most of the graphite exploration projects. In these types of settings, graphite enrichment may be a

consequence of two different phenomena; a) cooling of C-H-O-fluids or b) mixing of fluids derived from decarbonation-reactions in marbles or from paragneisses by the dehydration reactions. The fluids may also be derived from pegmatites or other small intrusions (Simandl *et al.* 2015).

There are two main ways in the formation of natural graphite. The first is the maturation of organic material that is later subjected to metamorphosis. The latter is the precipitation of graphite from metasomatic or metamorphic C-O-H-fluids. The general hypothesis for the origin of amorphous and low-grade crystalline flake graphite deposits can be explained by the maturation and metamorphosis of organic material. The process begins with carbonization and is followed by graphitization. The term 'graphitization' in a geological context is associated with the conversion from carbon-rich material into graphite (Simandl *et al.* 2015).

2.4 Graphite occurrences in Finland

Graphite is a relatively common mineral in the Finnish bedrock, but deposits of economic value are unusual. Between the years 1760-1947, 30 vein graphite deposits have been exploited in Finland. Today, 10 of these locations are on the Russian side of the border. From the 20 locations, altogether 1 800 tons of ore was enriched. Most of the mining occurred at Mäntyharju, Kärpälä approximately 150 kilometers SW from Aitolampi area (Ahtola & Kuusela 2015, Laitakari 1925). Ahtola & Kuusela (2015) have constructed a map where the known graphite deposits in southern Finland are plotted (Figure 4).

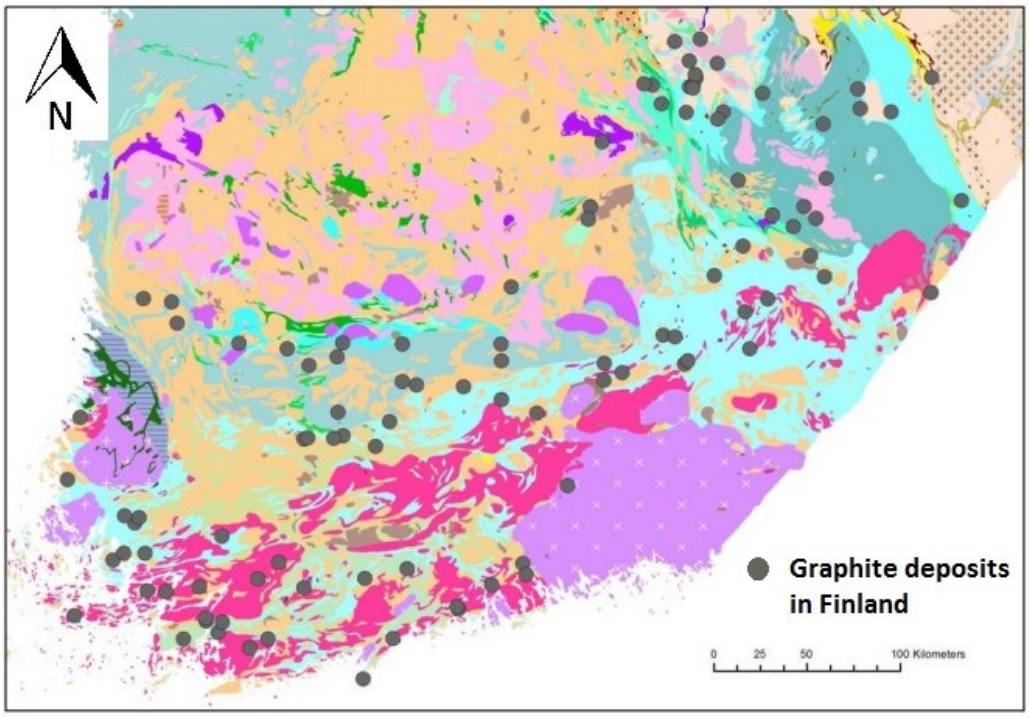

Figure 4. Known graphite deposits in southern Finland. Map based on Laitakari 's report on graphite occurrences in Finland (1925) with approximately 150 deposits. (Ahtola & Kuusela 2015)

Black schists in which most of the graphite deposits are located, are common in eastern and northern Finland due to the presence of 2060 – 1850 Ma old metasedimentary rocks. Most of the deposits are of vein type graphite, whereas the other deposits visible on the map are most likely lenses of amorphous or flake-type graphite in for example migmatites (Ahtola & Kuusela 2015).

2.5 Graphite enrichment in shear zones and fold hinge zones

Graphite may work as a lubricant in specific tectonic environments and the amount of graphite present has a big impact on the shear strength (e.g. Oohashi 2011). When folding occurs, compression takes place in the inner parts of the fold, whereas extension takes place in the outer parts (Figure 5). This leads to shearing and crack-forming and the material (e.g. graphite) may migrate in the inner parts if the environment and material is plastic and makes it possible. The pressure is lowest in

inner parts of the fold hinge zone and therefore an enrichment of the migrating material may occur in notable amounts.

Figure 5. During folding, the outer parts are subjected to extension whereas the inner parts are affected by compression. This leads to cracks and shearing and a possibility for the material to migrate towards lower pressures. (Pierce & Cosgrove 1990)

The migration of graphite towards lower pressures occur in a passive or an active way. The active way involves the presence of C-O-F- rich fluids. When the fluids are cooled down due to e.g. contact with the surrounding bedrock it can precipitate graphite (Figure 6, a). The temperature of the fluid has to be over 400˚C and the heat may origin from e.g. the friction in a shearing process. This can lead to cracks filled with graphite in contact to the shear zone. This has been documented in e.g. Atotsugawa fault zone, Japan (Oohashi 2011).

The passive transport of graphite includes a combination of *pressure solution* and *diffusional mass transfer* (Figure 6, b). Environments with higher pressure between the larger mineral grains can dissolve the graphite and later on are transported to areas with reduced pressures. The diffusional transfer involves transportation in a smaller extent; on atom or molecular scale. This transfer is due to the impurities that do not fit into the crystal lattice. When the temperature and/or pressure are increasing in the tectonic environment, it is possible for the impurities to migrate out of the lattice (Oohashi 2011).

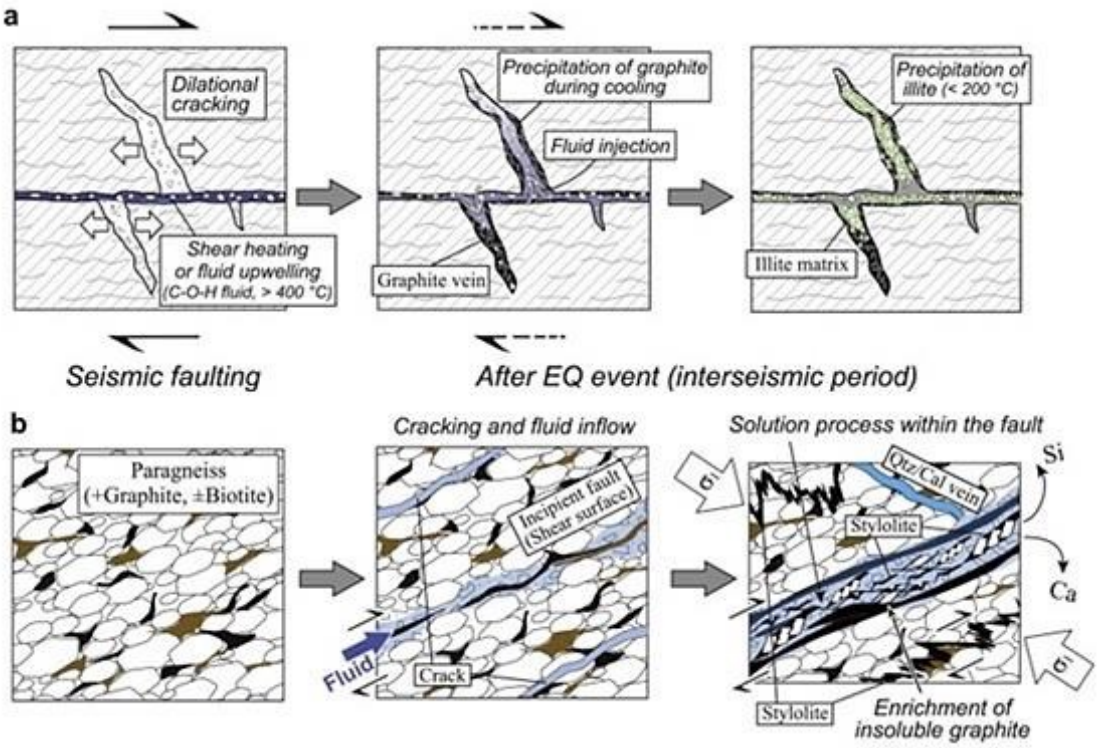

Figure 6. A visual representation of the passive (a, upper) and active (b, lower) way of graphite enrichment in shear zones. In the active way, the hydrothermal fluids are cooled down when in contact with the surrounding bedrock and thus precipitates graphite. In the passive way an enrichment of the insoluble minerals such as graphite is occurring. The water-soluble minerals are transported away with the fluids. Both examples from Atotsugawa fault zone in Japan. (Modified after Oohashi 2011)

According to Oohashi (2011), the original lithic composition may consist of very low graphite percentages (<3%) but still form graphite enriched areas in shear zones due to the migration of graphite.

In a study conducted by Henderson & Kendrick (2003), the structural controls on graphite mineralization has been studied in Troms, Norway. According to the study, the presence of graphite has a strong connection with the development of F_2 folds that have later on been deformed. The mineable graphite has mainly been present in fold hinge zones that have complex geometries in e.g. shear zones. In Troms, the graphite mineralization is spread over large areas as small lenses. The more exact location of graphite in F_2 fold hinges seems to be within the parasitic folds in the fold limbs or the M-folds within the fold hinge zone. Even more extensive graphite deposits can be found in areas that have been modified in terms of F_3 folding, preferably near shear zones (Henderson & Kendrick 2003).

Graphite's role as a lubricant is of great importance when constructing geological and structural settings in areas with possible graphite deposits. Enrichment of graphite may occur in the M-folds within the fold hinge zones (Figure 7) and in parasitic folds further away from the fold hinge zone (Henderson & Kendrick 2003).

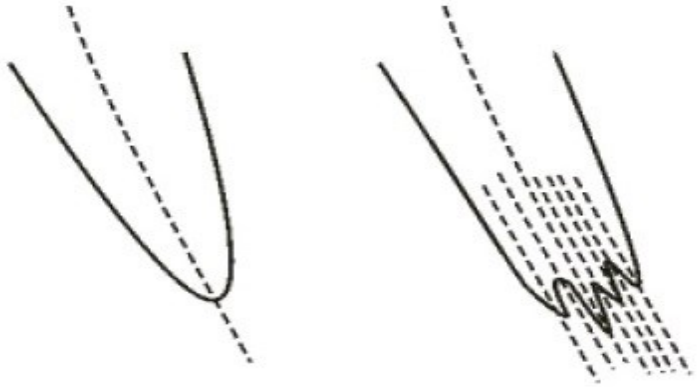

Figure 7. Structural re-interpretations of Krokelvdalen, Norway, deposit by Henderson & Kendrick (2003). The before-scenario (to the left) represents in structural terms a simple fold whereas the model to the right exemplifies the structures from a more recent study from the same deposit. The fold to the right consists of parasitic M-folds rather than a simple symmetric fold. (Henderson & Kendrick 2003)

3. GEOLOGICAL OUTLINE

3.1. Regional geology

The Finnish bedrock is composed to a third of the Fennoscandian bedrock. The northern and eastern part of Finland belong to the 3100- 2500 Ma Archean bedrock (Figure 8). The southern and central parts belong to the early Proterozoic bedrock with an age from 1930 – 1800 Ma. Only a minor part of the bedrock in Finland is younger than 1800 Ma. The only major formation after this has been the formation of 1650 – 1540 Ma Rapakivi- granite batholits. Most of the Svecofennian rocks are 1905 – 1880 Ma, but the metavolcanites in Savo schist belt are slightly older, 1930 – 1920 Ma old (Kähkönen 1998; Laajoki 1998).

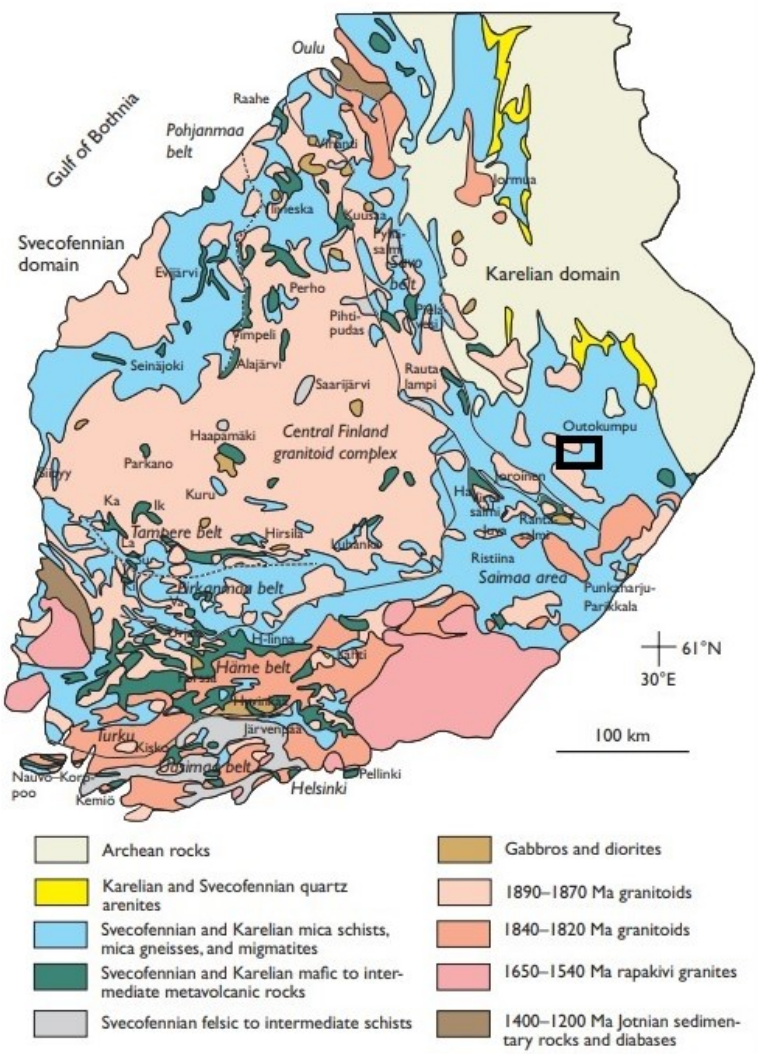

Figure 8. A general overview of the geology of southern part of Finland. Aitolampi area is marked with a black box on the map. (Kähkönen 2005)

The Svecofennian bedrock is mainly composed of metasediments that have been metamorphosed to phyllites, mica schists, mica gneisses and migmatites. The Svecofennian bedrock is also composed of granitic intrusions and mafic metavolcanites with an association of island arc volcanism (Kähkönen 1998). Several different types of volcanites are present between the metasediments. Black schists are present as layers and lenses in paragneiss and metapelitic rocks, mostly in eastern Finland (Kähkönen 1998).

The peak of the metamorphosis is within the upper amphibolite facies, 650-700˚C and 4-5 kbar (Kähkönen 1998). The lower metamorphic facies varies in the zone between amphibolite- and greenschist facies, ~500 ˚C and 3-5 kbar (Kähkönen 1998).

Due to younger faults and folds, the area is divided into several smaller parts in regards of metamorphism (Figure 9). This is because the metamorphic degree may have variations within a relatively small area (Kähkönen 1998).

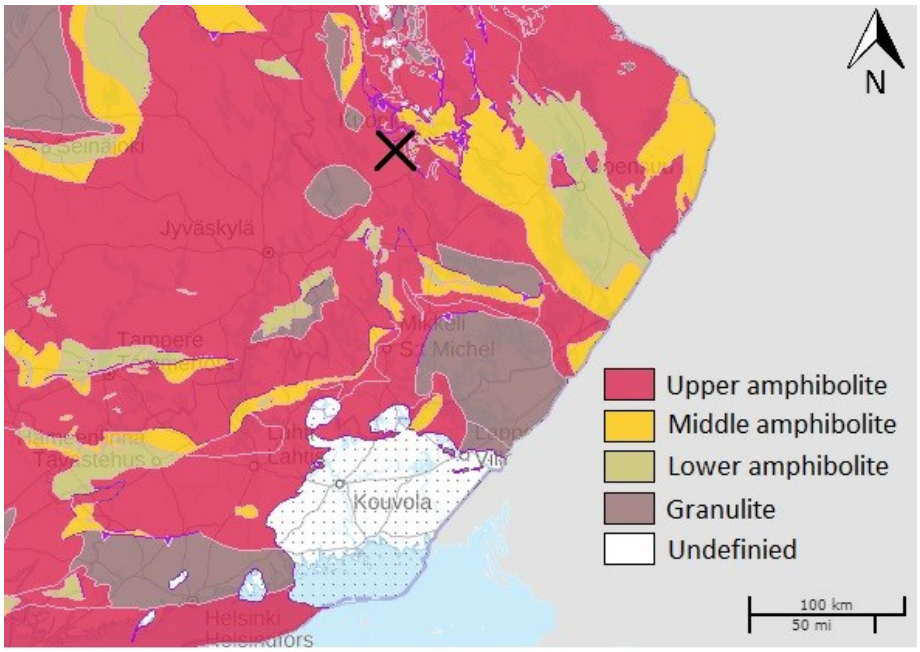

Figure 9. A metamorphic map of southeastern Finland. Aitolampi study area, marked with a black cross, is a part of the upper amphibolite metamorphic facies. (Hölttä & Heilimo 2017)

Lines 3 and 3A within the Finnish Reflection Experiments (FIRE) are of interest in this study, due to the close location to the study area (Figure 10). The experiment has divided areas into different crustal domains based on the seismic variations concerning structural and lithological variations (Sorjonen-Ward 2006). Aitolampi area has been categorized to the Suvasvesi domain, located west of Outokumpu domain, east of Unnukka domain and south of Kuopio domain. Typical for the Suvasvesi domain is the interaction between crustal scale shear zones and granitoids and the high-grade metamorphism of passive margin sediments with buried mantle-derived granites and migmatites interacting with granite emplacement. Post –Svecofennian reactivation can be observed from the area (Sorjonen-Ward 2006).

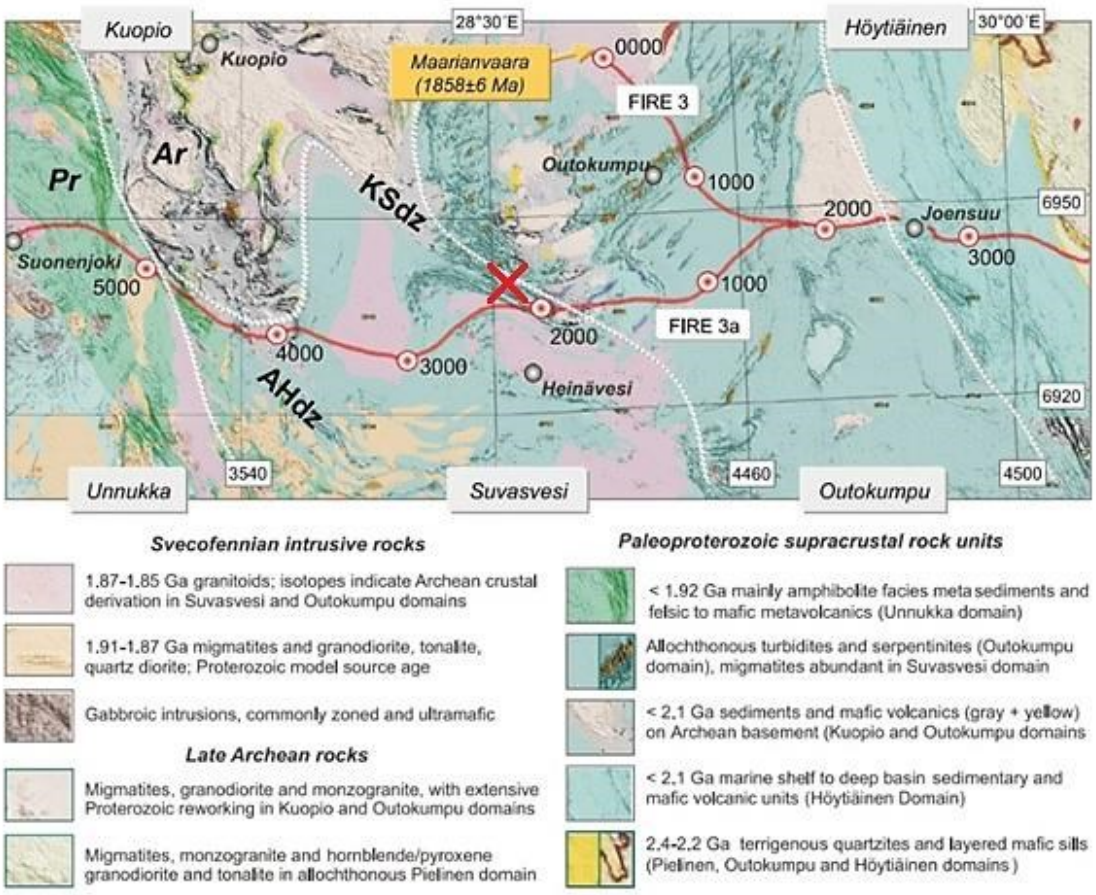

Figure 10. FIRE 3 – and 3A-lines in the lithological map. KSdz = Kallavesi – Suvasvesi deformation zone, AHdz = Airaksela – Haukivesi deformation zone. Aitolampi study area is marked with a red cross. (Sorjonen-Ward 2006)

The study area is on a regional scale located in the North Karelian Schist Belt (NKSB) in eastern Finland (Figure 11). The NKSB can be divided into two tectonic provinces based on the differences in depositional settings; Savo and Höytiäinen province (Ward 1988).

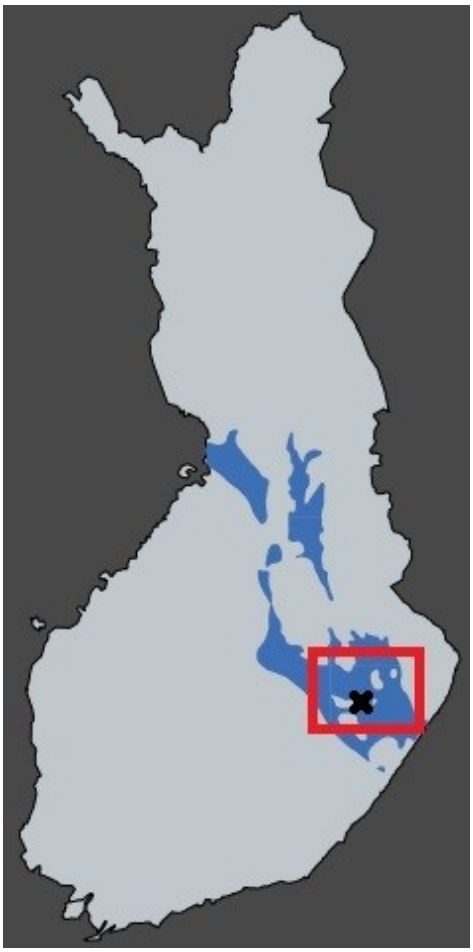

Figure 11. The red box indicates the location of the North Karelian Schist Belt. The dark blue areas represent the Karelian formations in Finland according to Laajoki (1998). Aitolampi study area is marked with a black cross.

The NKSB is a part of the Karelian supergroup that is comprised of both allochthonous and autochthonous sedimentary sequences from the Paleoproterozoic platform (Sorjonen-Ward 2006). This Karelian supergroup separates the Paleoproterozoic domain towards west and south and the Archean domain in the north and the east (Ward 1988). The Karelian domain can be considered as the cratonic nucleus to the Fennoscandian Shield. This is due to the Karelian domain acting as a foreland to which the Svecofennian nappes were thrusted 1900 Ma ago (from SW) (Laajoki 1998).

3.2 Aitolampi local geology

On a more local scale, the Aitolampi study area is a part of the Karelian domain of the NKSB, consisting of Paleoproterozoic supracrustal rocks. Metasediments deposited in different environments are typical rocks in this area. The depositional settings have varied from deep ocean basins to continental shelves (Laajoki 2005). Turbiditic features in the massive psammitic rocks are typical for the metasediments in Savo domain (Ward 1988). The sedimentation rate has been fast due to presence of occasional load casts. Fast occurring sedimentation is typical for environments such as delta or continental shelves (Ward 1988). The sedimentation has been dated to 2500 – 1900 Ma and the deformation has been taken place between 1900 – 1800 Ma (Vuollo & Huhma 2005).

Biotite paraschist is a dominating rock type in the Aitolampi study area (Figure 12). It consists of quartz, plagioclase feldspar, micas (dominantly biotite) and +/- graphite. Garnets and chlorite are typical accessory minerals. Graphite is present within the black schist in gneisses as lenses and layers. The possible black schist areas are presented in Figure 12. The bedrock has a weakness-zone in a NW-SE-direction.

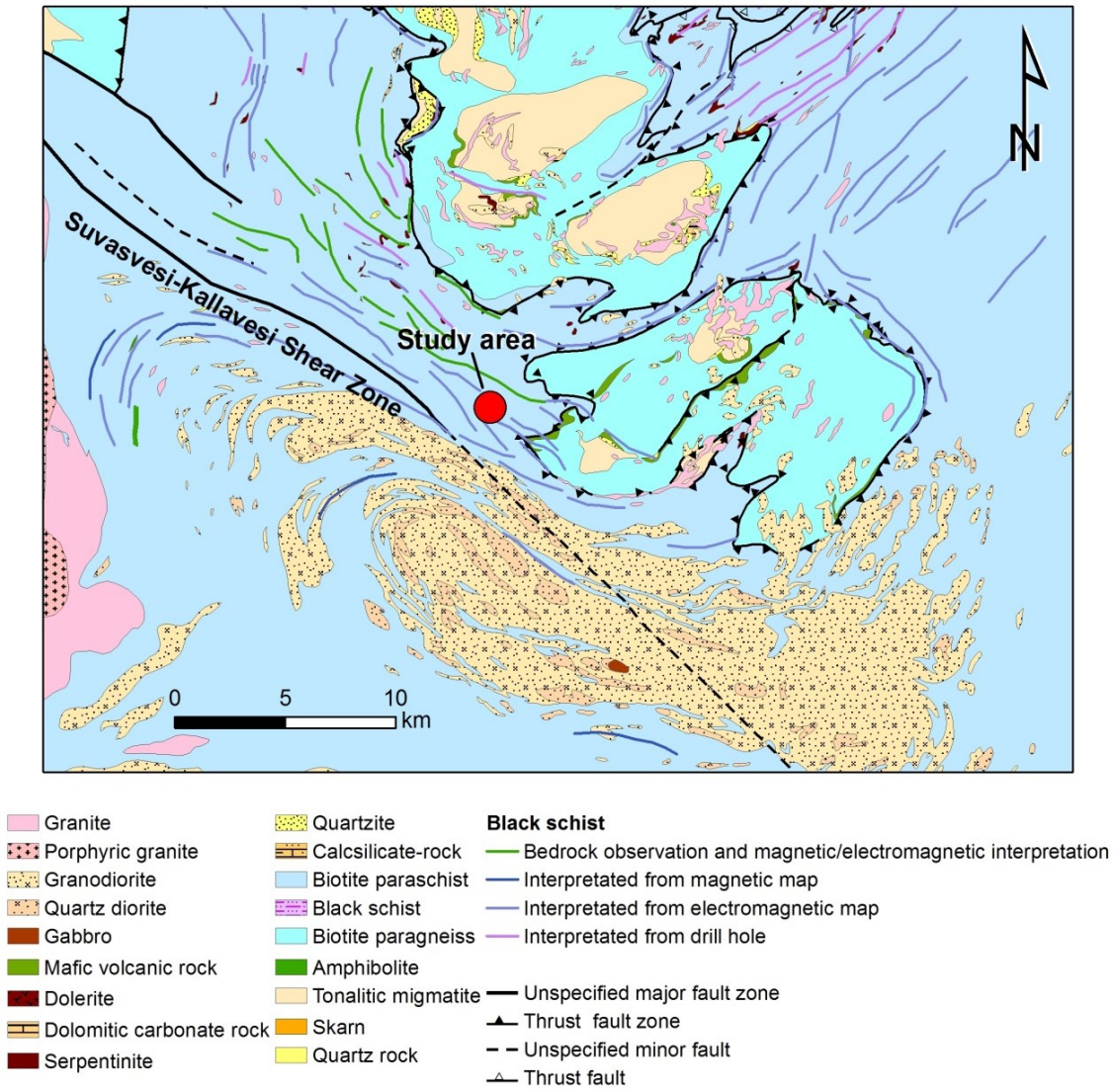

Figure 12. Bedrock map of the study region. The map includes the interpreted occurrences of black schist (green, blue and purple lines) by GTK. The thrusts, mainly composed of biotite paragneiss (bright turquoise) represent the Outokumpu nappe complex. (Bedrock 1: 200 000, Geological Survey of Finland 2017)

GTK (Geological Survey of Finland) has been conducting systematic airborne, low-altitude electromagnetic, magnetic and radiometric surveys covering most of Finland during 1972 – 2007. The flight altitude has varied between 30-40 meters with main line spacing of 200 meters (Airo 2005). The data has been used in the FennoFlakes project to identify potential areas of interest.

Beowulf Mining plc has carried out electromagnetic Slingram measurements which can also be called ground HLEM (Horizontal Loop Electromagnetic) measurements, in

the study area during 2015 and 2016 in order to better localize areas of possible graphite mineralization. Geological mapping and outcrop sampling have also been conducted.

3.3 Haapamäki

A large-scale synformal fold is located south from the study area (Figure 13). This fold is called the Haapamäki fold and it is 10 kilometer wide and 25 kilometers long and can be observed from aeromagnetic anomaly-, bedrock- and airborne electromagnetic maps. Kallavesi-Suvasvesi deformation zone (KSdz) is located between Aitolampi area and Haapamäki fold.

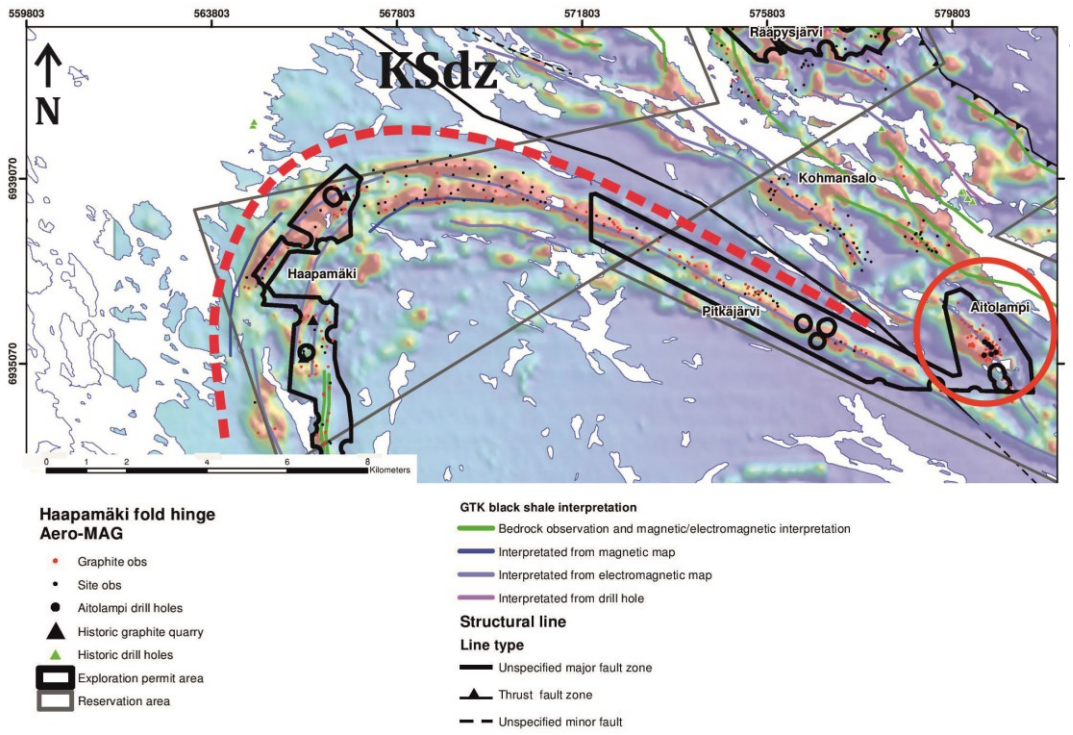

Figure 13. Haapamäki fold on an aeromagnetic map (dashed red line). Hot colors indicate elevated conductance. KSdz is located between Haapamäki fold and Aitolampi area. Red circle marks the Aitolampi study area. (Modified after Beowulf Mining plc)

The Haapamäki fold is partly consisting of biotite paraschist with large areas of grano- and quartzdiorite. The main rock type in Haapamäki is migmatite which can in places be strongly folded. Ptygmatic folding (irregular folds with curved axial planes)

and boudinage has been identified in some places. Graphite is present in various amounts. Black schist is presents as long lenses (horizon-like) within the migmatite (Nygård 2017).

Graphite has been known to occur at Haapamäki since the late 1800´s. Graphite has been mined mainly in three different localities in the Haapamäki between the years 1870 - 1880. Laitakari (1925) has reported these locations, which are; Kultakallio (1), Käärmerinne (2) Suurenkahanvuori (3) (Figure 14).

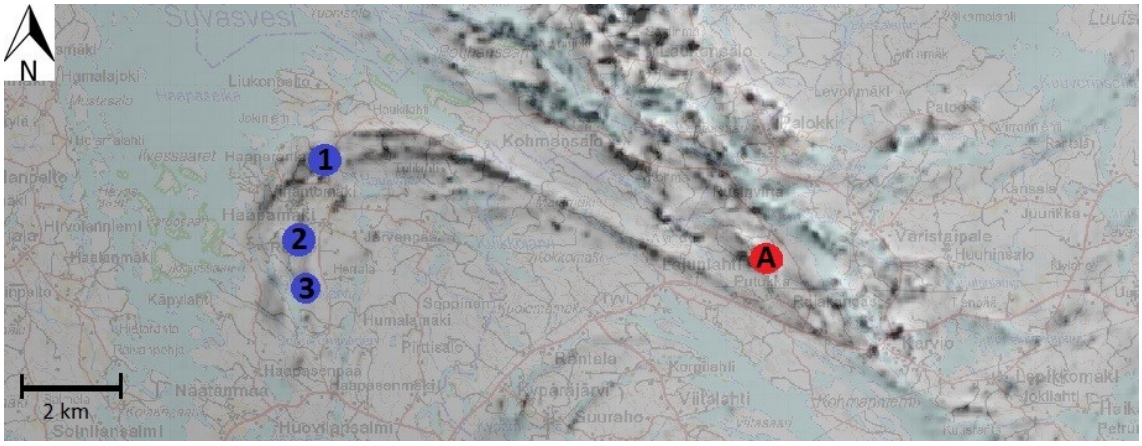

Figure 14. The old graphite deposits in Haapamäki are located in the fold hinge zone. The three blue dots (1,2,3) mark the old mining locations and A the Aitolampi study area. (Modified after National Land Survey of Finland 2013)

According to Nygård (2017) the passive transport and enrichment of graphite can be observed from Suurenkahanvuori deposit, located near the fold hinge zone in Haapamäki (Figure 14). Characteristic shearing structures such as mylonitic shearing with the typical elongated grains can clearly be observed (Nygård 2017).

4. MATERIAL AND METHODS

4.1. Slingram

Slingram is an electromagnetic method used to measure the conductivity of bedrock. The advantage of EM methods is that they do not require a contact with the ground. There are different types of Slingram methods, with variations in e.g. penetration depths. In the study area, two types of Slingram measurements were conducted.

The Slingram EM system consists of 2 co-planar horizontal transmitter (Tx) and receiver (Rx) loops, with a 60m Tx-Rx separation and uses a frequency of 3.6 kHz. In idyllic conditions, the Slingram has a penetration depth of half the length of the cable (between Tx and Rx), which in this case would mean a penetration depth of 30 meters (Beowulf Mining plc). Mini-Slingram survey has Tx-Rx loops oriented 55 degrees from horizontal and the loop separation is approximately 1,5 meters. The frequency for Tx is 5 kHz. The mini-Slingram method has a shallower penetration depth than Slingram due to the smaller Tx-Rx loop. The penetration depth for mini-Slingram in idyllic conditions is up to 26 meters (Beowulf Mining plc). By combining both of the methods, more conductance data is gained.

The two types of measurements conducted in the Aitolampi study area were the Slingram Frequency-Domain Electro Magnetic (SFDEM) or 'Slingram' and the Mini-Slingram Frequency-Domain Electro Magnetic (MSFDEM) or 'mini-Slingram'. Slingram measurements penetrate deeper than the mini-Slingram measurements. By comparing and combining both of the methods, sharper and more distinct anomalies are gained (see Appendix A). Slingram gives broader and "smeared" anomalies, whereas mini-Slingram gives smaller anomalies, due to the shallower penetration depth.

The most conductive areas are located as parallel lines in a NW-SE direction in Aitolampi study area (Figure 15). The conductivity of graphite schist increases with grade, flake size and thickness of the layer.

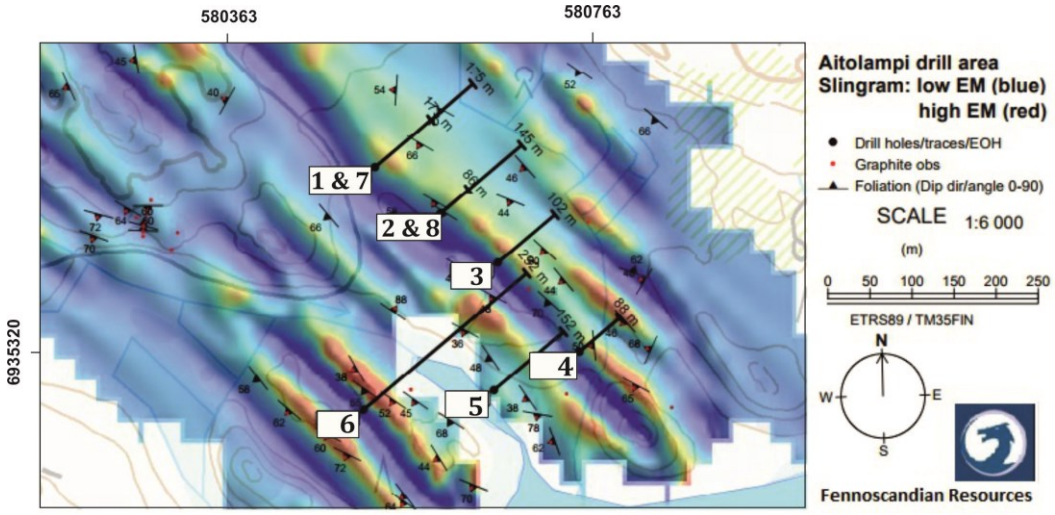

Figure 15. Slingram measurements in Aitolampi. Hot colors represent zones with elevated conductance. The black lines represent the drillholes, drilled towards NE. (Modified after Beowulf Mining plc)

4.2 Field work

The detailed bedrock mapping of the drilling area was made in May 2017. The aim of the detailed structural mapping was to measure structures, map the bedrock and build on previous structural and lithological data from Aitolampi area.

The mapping was conducted together with Exploration Geologist Sauli Raunio (Beowulf Mining plc). Rock samples were taken with a rock hammer and sampled into bags, ranging from 1-5 kg. The graphite-bearing rocks were in main focus when sampling. Sampling of the side rock was also done, in order to gain a better understanding of the petrography.

It was important to sample the surrounding bedrock in order to correlate the rock types from the bedrock mapping with the rock types from drill cores. Altogether 30 outcrops were mapped. From previous years 48 mapped outcrops could be utilized when interpreting the drilling area. The coordinates for the observations can be seen from Appendix B.

4.3 Diamond drilling and core logging

Altogether 1150 meters were drilled in Aitolampi in February/ March 2017. There are eight drill holes in Aitolampi area, drill holes 1 and 7 have the same starting point as well as drill holes 2 and 8 (Figure 15). They have been drilled with different dips towards the same direction. The cross cuts from drill cores are presented in Appendix C.

The planned azimuth for all of the drill holes was 050 degrees, which is perpendicular to the dominating foliation in the area (based on bedrock observations). The planned dip was 30 degrees for drill holes 1-6, and 60 degrees for drill holes 7 and 8. The diamond drill was of size WL76 in order to make possible a large and sufficient sample size for metallurgical tests from the drill cores. This means that the width of the drill core is 76,3 millimeters. Exact azimuths and dips were given later on by the drilling company (Appendix D), since drill holes are usually curved, due to the variations in lithology causing differences in competence and hardness. The corrected values were taken into account during interpretations in later stages. The starting points for the drill holes on the surface are indicated in the collar table seen in Appendix D. A collar table includes a collar ID (drill hole), the location of the drill hole in X, Y, Z coordinates and the maximum depth/ end of drill hole.

The structures measured from the drill cores were drawn into 2D cross sections based on the foliation measurements conducted with a goniometer. The geological logging and geotechnical measurements of the cores, which has been used in this thesis, was done by Rasmus Blomqvist, Sauli Raunio, MSc student Henrik Nygård and the author. The geotechnical measurements included RQD, density- and structural measurements.

4.4 Stereographic projections

The Stereonet- software by R.W. Allmendinger v. 9.8, was used for stereographic projections. The data used in the projections was the measured foliations of quartz-feldspar-biotite gneiss (QFB gneiss) and graphite schist. After studying the foliation

data, measurements taken beside or near fracture zones and pegmatite dykes were removed from the stereographic projections.

A stereographic projection was made from each drill core and one common projection from the field observations in Aitolampi. As reference material, a projection was made from field observations from Kohmansalo, an area located 8 km NW from Aitolampi on the same (northern) side of Kallavesi-Suvasvesi deformation zone.

5. RESULTS

5.1 Fieldwork

The main rock type in the mapped area is quartz-feldspar-biotite gneiss (QFB) and graphite schist. In the field, the name graphite schist was used if the amount of graphite present appeared to be at least 3%. The measured foliations have an average strike of 218˚, varying between 200˚ and 260˚ apart from a few exceptions. The average dip is 58˚, with variations from approximately 40˚ to 80˚ (towards NW/NNW).

During bedrock mapping, pegmatite dykes were observed to cut the study area in several different directions. Some of the observed pegmatite dykes may also be part of the leucosomes from migmatites. The leucosomes may in some cases behave like pegmatite dykes and cut fold axes and other structures even perpendicularly (e.g. oral communication with Karin Högdahl, UU, 12/2017).

5.2 Stereographic projections

According to the stereographic projections constructed from Aitolampi, there are two fold axes trending with approximately an 180˚ difference. For drill holes 1,2,3,5 and 6 the fold axis is present towards NNW, the values for the trend is varying from 342-348˚. For drill holes 4, 7 and 8 the stereographic projections point to a fold axis located towards SSE, with trend values varying from 156-164˚. The stereographic projections

for drill holes 1-8 are presented in Figures 16 and 17. Drill holes 1 and 7 as well as 2 and 8 are presented here side by side, since the starting point for the drilling is the same; plunges are different (40˚ respective 60˚). Drill holes 3 and 6 are also side by side, since they are drawn in the same cross section, but do not have the same starting point for drilling. See Appendix C for illustration.

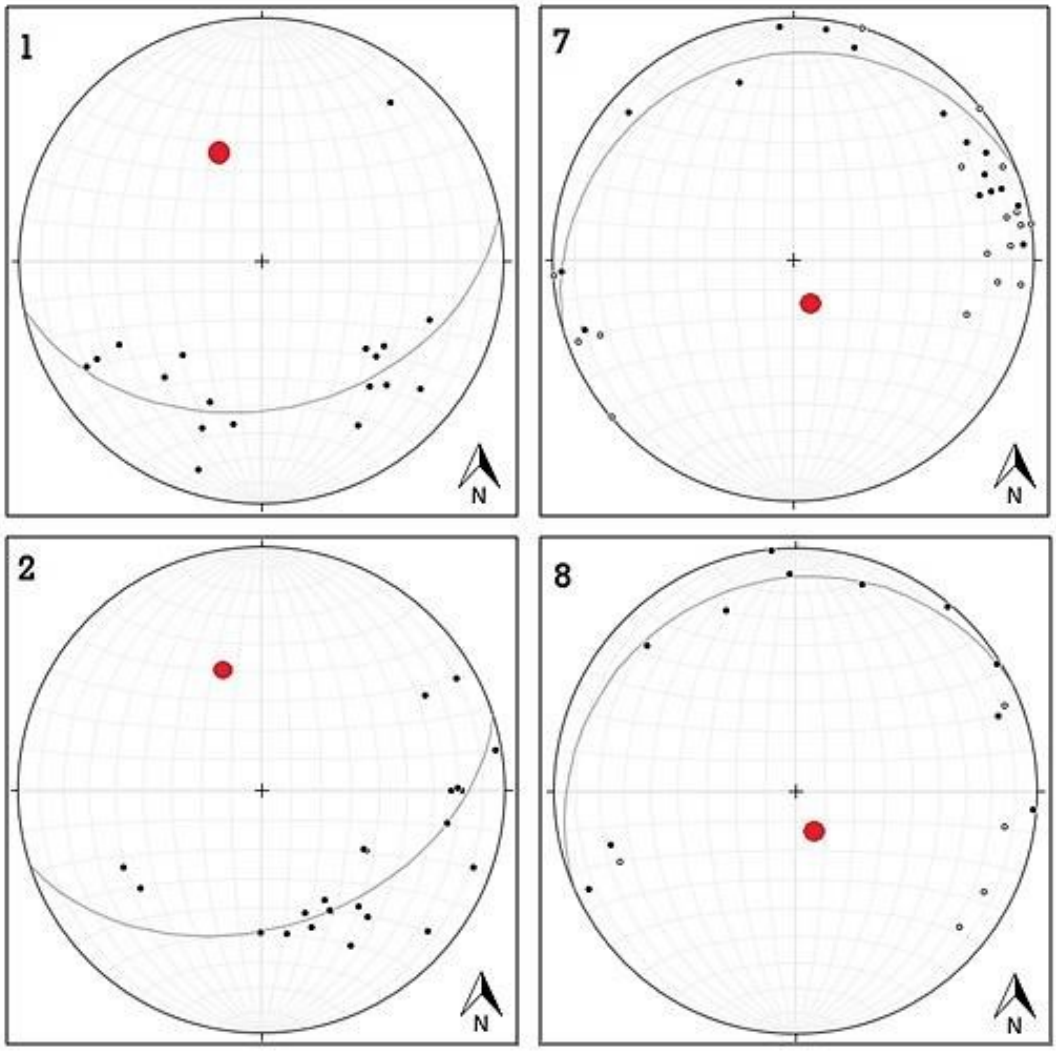

Figure 16. Stereographic projections for drill holes 1,7,2 and 8. The black dots are poles for foliation measurements of QFB and graphite-schist. The red dot represents the calculated fold axis. Stereographic projection for drill hole 1; the calculated fold axis 348/38 (DD/D). The strike/dip for this plot is 078/38 (top left). Stereographic projection for drill hole 7; the calculated fold axis is 164/16 (DD/D). The strike/dip for this plot is 252/16 (top right). Stereographic projection for drill hole 2; the calculated fold axis is located 342/43 (DD/D). The strike/dip for this plot is 072/43 (bottom left). Stereographic projection for drill hole 8; the calculated fold axis is 156/14. The strike/dip for this plot is 245/14 (bottom right). (Stereographic projections constructed with Stereonet by R.W. Allmendinger)

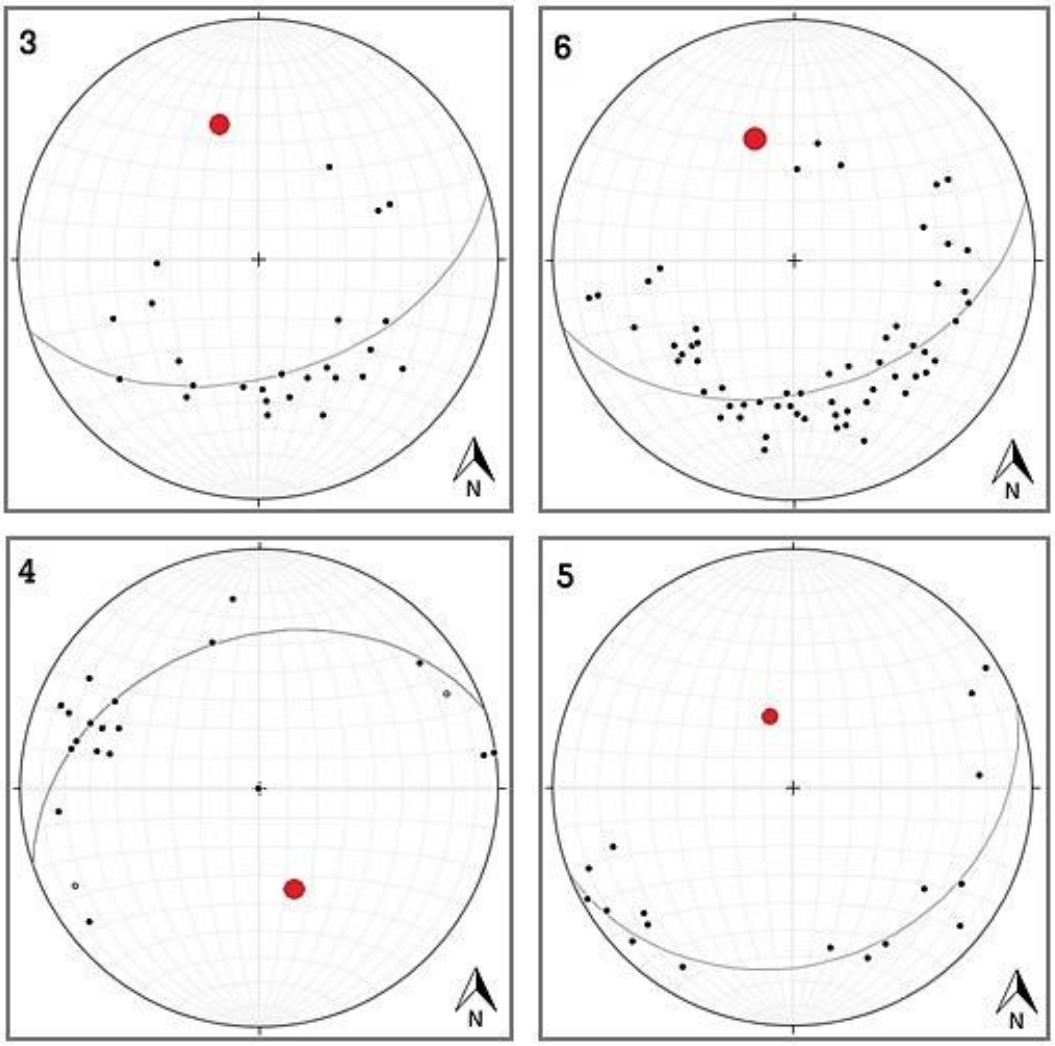

Figure 17. Stereographic projections for drill holes 3, 6, 4 and 5. The black dots are poles for foliation measurements of QFB and graphite-schist. The red dot represents the calculated fold axis. Stereographic projection for drill hole 3; the calculated fold axis is 343/50 (DD/D). The strike/dip for this plot is 073/50 (top left). Stereographic projection for drill hole 6; the calculated fold axis is 344/44. The strike/dip for this plot is 074/44 (top right). Stereographic projection for drill hole 4; the calculated fold axis is 161/37 (DD/D). The strike/dip for this plot is 250/37 (bottom left). Stereographic projection for drill hole 5; the calculated fold axis is 340/27 (DD/D). The strike/dip for this plot is 070/27 (bottom right). (Stereographic projections constructed with Stereonet by R.W. Allmendinger)

Stereographic projections from Kohmansalo and Aitolampi (Figure 18) have approximately the same calculated fold axes as drill holes 1,2,3,5 and 6; pointing towards NNW.

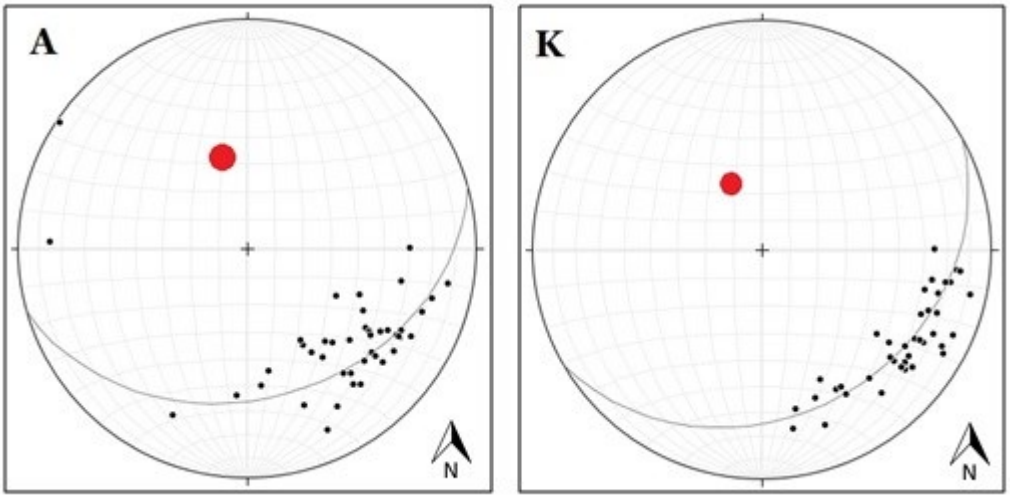

Figure 18. Stereographic projections based on field measurements from Aitolampi (A, left) and Kohmansalo (K. right). The calculated fold axis for A is 344/35 (DD/D) with a strike/ dip 073/35. The calculated fold axis for K is 331/28 (DD/D) with a strike/ dip 060/28. (Stereographic projections constructed with Stereonet by R.W. Allmendinger)

6. DISCUSSION

6.1 Slingram

Several factors have an impact on the effectiveness of Slingram-measurements: porosity, humidity and salinity of the ground (Peltoniemi 1988). Minerals have varying electrical conductivities and therefore variations in the bedrock are seen in the data. It is also important to take into account electrical cables in the air or in the ground, pipelines or other metallic objects that may cause disturbances in the data (Peltoniemi 1988).

The theoretical penetration depths for Slingram measurements are most likely not realistic, since the effectiveness depends of the electrical resistance of the ground. When the ground is more resistive, the Slingram may penetrate even deeper than half of the cable length. A more realistic penetration depth is approximately ⅓ or ¼, of the

cable length, which in this case would mean a depth of 15-20 meters for the Slingram and for the mini-Slingram 10 meters (Sami Niemi, GTK, oral communication, 2/2018).

Sulphides are good conductors and e.g. pyrite is present in the drill cores and was observed during bedrock mapping. Therefore, some of the EM-anomalies may be caused of the presence of other conductive minerals than graphite. When bedrock mapping was conducted, some samples and boulders with an elevated amount of graphite were observed from the non-conductive areas according to Slingram data.

The qualities of the bedrock and the ground are an interesting factor when it comes to EM measurements. Even if moraine itself is not conductive, it has an effect on the measurements. Graphite layer(s) present beneath 1 meter of moraine are better "seen" by the Slingram compared to those buried under 20 meters of moraine/ glacial deposits. The amount of graphite and the thickness of the graphite bearing layer(s) must also be taken into account. A heavily enriched graphite-layer may give very strong anomalies from relatively deep from the surface. In the Aitolampi area, parts of the area are swampy and therefore the water content in the ground is higher than on average. Bottoms of swampy areas are very conductive and the electrical current may get "stuck" to the topmost conductive layers (Sami Niemi, GTK, oral communication, 2/2018). Therefore the possible graphite present beneath these swampy areas is not necessarily seen in the Slingram data.

6.2 Fieldwork

At a few sites the graphite concentration was estimated to 4-5% (Figure 19, left). Graphite schist is generally fine-to-medium grained and mostly moderately foliated. The graphite is mostly present as disseminated 0.1-0.5mm and 0.5-1mm flakes. In some sites, the graphite is concentrated in patches together with biotite. The graphite-bearing black schist in the area is present as layers within the QFB-gneiss. In some areas, the occurrence of graphite could be identified when "smoothing out" the edges of a sample by hand and seeing the shiny and smooth surface caused by the soft graphite.

In general, a good indicator of graphite in the field is the rusty and weathered outcrops (Figure 19, right). In some sites where graphite is present, the sulfide concentrations were estimated to 3% or slightly higher. When the sulfur concentration was >5%, the S-rich minerals were present as stringers (narrow veins) in the host rock.

Figure 19. A sample of the graphite schist, with an estimated 4-5% of graphite (left). A typical view of an outcrop during bedrock mapping, the rusty appearance usually went hand-in-hand with presence of graphite (right).

Strong deformation and migmatite-like structures disturbed some of the structural measurements in places.

Pegmatite dykes and smaller quartz-plagioclase veins are often present beside the graphite-bearing schist on the same outcrop (Figure 20). Elevated percentages of graphite were usually observed near these kinds of outcrops.

Figure 20. A pegmatite dyke cutting through the graphite schist.

Boudines and shearing patterns (e.g. mylonitic structures) are visible at some sites. The most apparent deformation is located in the northeastern part of the mapping area, away from the aeromagnetic anomalies. In this area, mylonitic structures are present along with very large and coarse pegmatite dykes.

The degree of metamorphism has local variations, which can be interpreted by the presence of garnets in the bedrock, dominantly in the QFB gneiss. The QFB gneiss was both garnet-rich and garnet-bearing (G-QFB) depending on the local metamorphic variation.

6.3 Drill core orientation

Before making the structural measurements from the drill cores, the cores were oriented by the Beowulf Mining plc geologists. When the drill cores were oriented some differences in the continuation of orientations were noted. The foliation measurements from the drill cores were in places clearly deviant from the surrounding measurements. The differences in orientations varied from <10˚ up to 180˚. Big

differences in the orientation of drill cores do not give reliable results. On the other hand, the foliations in the bedrock may also have big variations within relatively small areas. When interpreting the data some uncertainties with the core orientation were present during the work. In general, the orientation results are considered trustworthy.

6.4 Stereographic projections

The fracture zones and pegmatite dykes may have had a heavy effect on the foliation and therefore affect the measurements made from the drill cores. The removal of the measurements taken beside fracture zones and pegmatite dykes was done because the size of the area affected by them is hard to predict by only studying the drill cores. This was made in order to get as authentic stereographic projections as possible and to minimize the risk of misleading measurements being present. The pegmatite dykes are most probably younger than the QFB-gneiss (field observation) but older than some of the deformation they have been subjected to. Some boudinage-structures were observed in the field and they were noted to cause bending of the dominating foliation towards the boudines (Figure 21). Therefore they may have formed pressure shadows or secondary foliation due to deformation and thus show a “false” foliation. The fracture zones and pegmatite dykes may have had a similar effect and thus cause a false foliation.

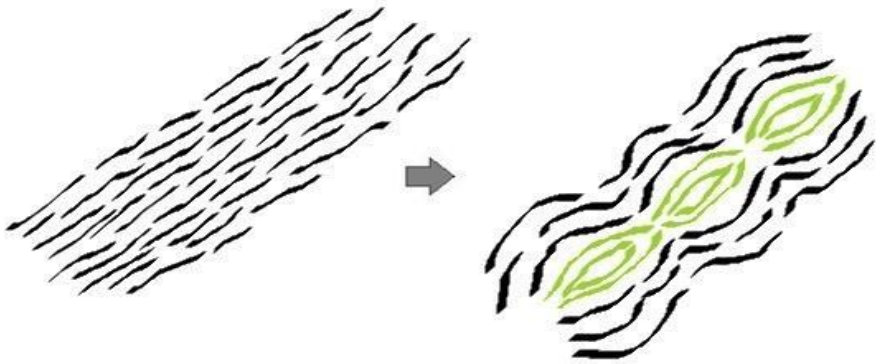

Figure 21. The original foliation in the area is illustrated to the left. An intrusion of e.g. a pegmatite dyke (green) followed by deformation may have caused boudines and secondary foliation adapting to the boudines (right).

6.5 Graphite enrichment

Henderson & Kendrick (2003) have concluded that graphite can be enriched to fold hinge zones and the parasitic folds located further away from the hinge zone. Based on Slingram measurements and the cross cuts from drill cores in Aitolampi that theory seems to fit the study area. Parasitic folds are common in areas with ductile deformation and may cause complex geometries (Henderson & Kendrick 2003). The fold hinge may consist of several parasitic M-folds (Figure 22) as discussed earlier. The presence of graphite is a factor whose effects cannot be calculated with models; graphite is mobile and works as a shear strength lowering factor (e.g. Henderson & Kendrick 2003).

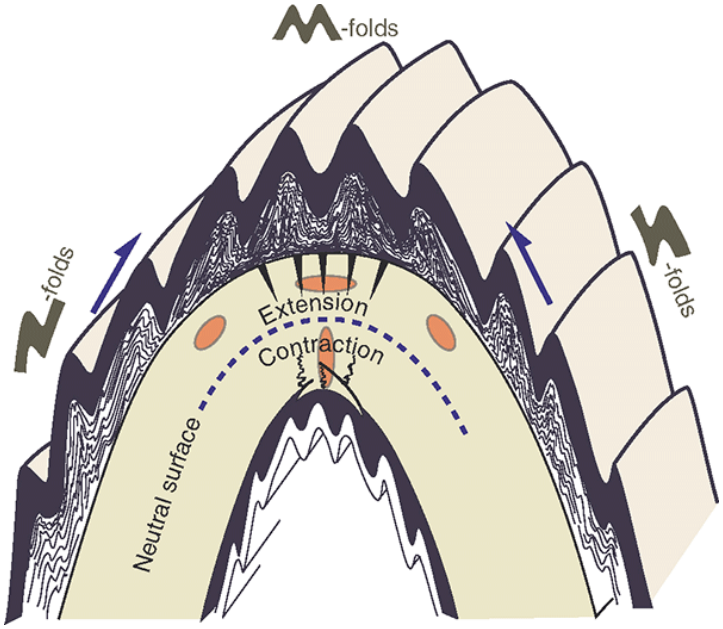

Figure 22. A sketch of an antiformal fold, the M-folds are located in the hinge zone. The parasitic folds are located towards the limbs of the fold. (Fossen 2011)

The highest grades of graphite are present in the antiforms, due to the gravitational effect making it is easier to migrate upwards than downwards with e.g. the fluids. The synforms may in some cases be enriched in graphite, but this may be a consequence of the graphite-bearing layer itself. During the sedimentation and deposition, a layer may have been very rich in organic material that would later on be converted into graphite. After the deformational events and folding, this enriched layer located in a synform

might have even lost some of the graphite due to migration and is now poorer, but still graphite-bearing (Figure 23, left). Another explanation for graphite enrichment in synforms is that the graphite has been present as small but graphite-rich horizons that have due to the extension only been stretched and no graphite migration has occurred. In both scenarios, the amount of graphite is the same but the dispersion is different.

The enrichment of graphite into antiforms may be a consequence of the migration of graphite into lower pressures in a fold hinge zone, as stated earlier (Figure 23, right).

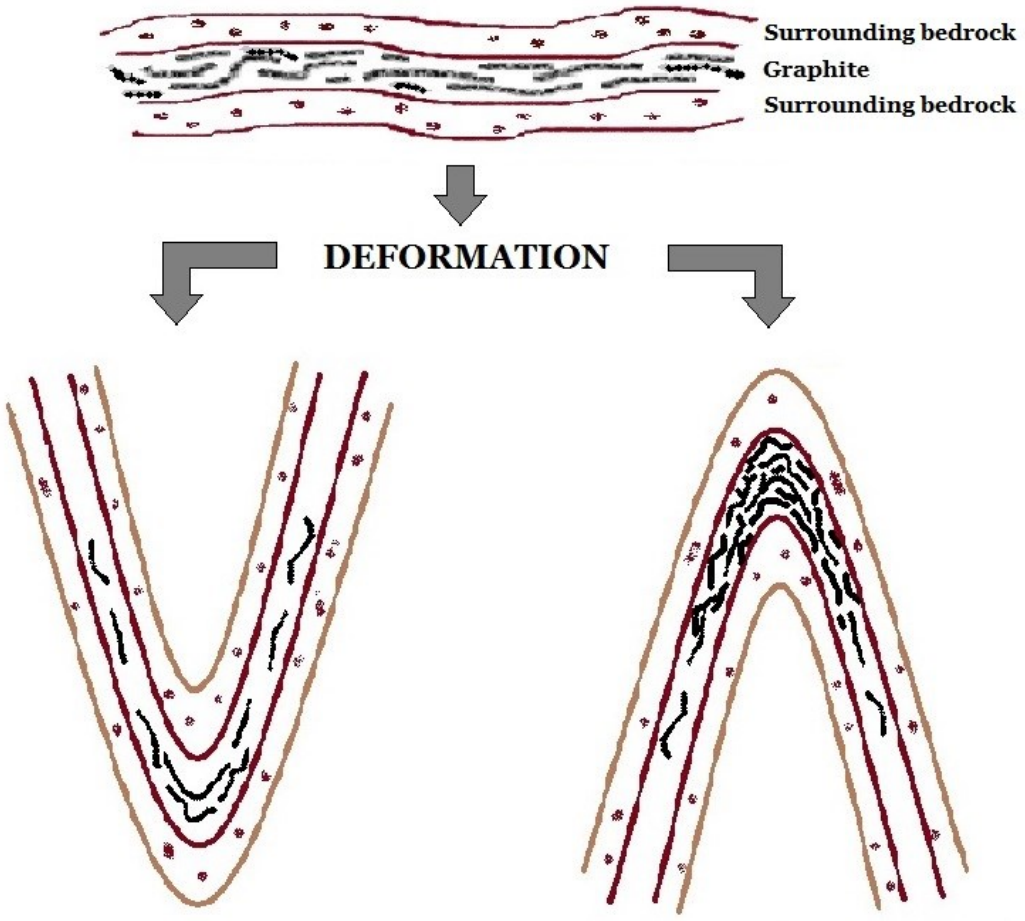

Figure 23. A schematic illustration of the graphite-bearing layer being subjected to deformation (folding). The black lines represent graphite and the brown layers the surrounding bedrock. The graphite in the synform (left) is migrating upwards when subjected to deformation, but there is still graphite remaining in the fold hinge zone. The enrichment may also be caused by the elevated amounts of graphite already present in the layer, now extended to a wider area. In the antiform (right), the graphite is migrating towards the lower pressures in the fold hinge zone when subjected to deformation, thus enriching the hinge zone.

What this points to is that black schist layers containing relatively low amounts of graphite may become enriched in graphite after deformational events (e.g. to the antiforms) as stated by Oohashi (2011). The case may also be the opposite, graphite-rich areas may be subjected to deformation so that graphite can migrate away (e.g. from the synforms). Therefore, it is of major importance to understand the relationship between structural events and individual graphite deposits in the area.

6.6 Local structural setting

The Slingram measurements show clearly a pattern with the conductivity in the area: somewhat continuous "lines" in a SE –NW direction (Figure 24). These lines have small-scale discontinuities; the reddish colors indicating elevated conductance is not evenly spread within the lines (Figure 24, yellow box). The lines are partly consisting of non-conductive areas, marked with blue color.

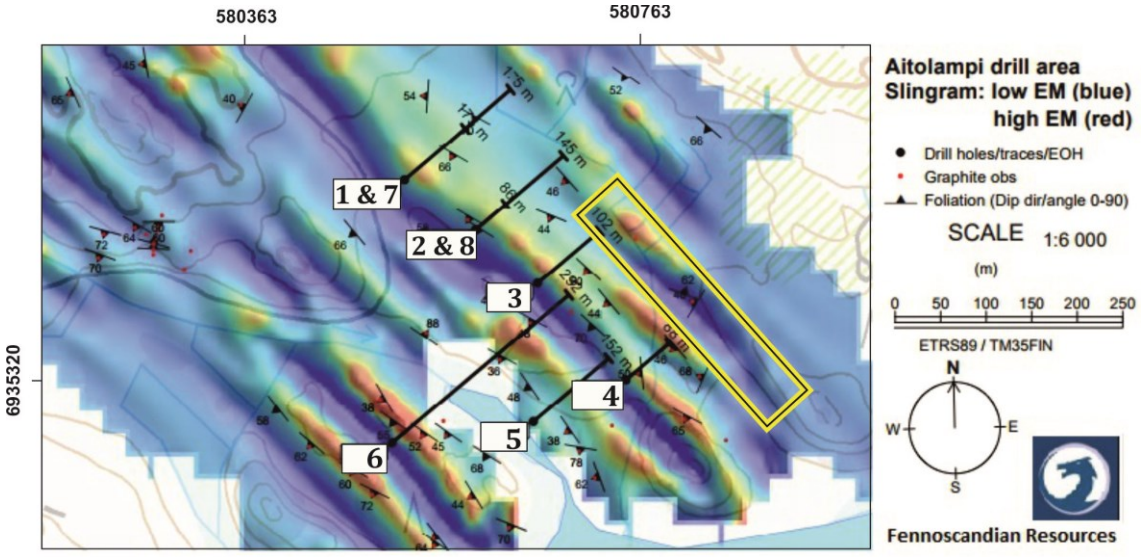

Figure 24. The Slingram-map over Aitolampi, where the reddish colors represents elevated conductance. The yellow box marked on the map represents the variation in conductivity within one EM line in a NW-SE direction. (Modified after Beowulf Mining plc)

As mentioned earlier, two calculated fold axes/ beta axes were found. These have opposite plunges and can thus be interpreted as an antiformal double-plunging structure in the area. A double-plunging antiform is a non-cylindrical fold (Figure 25).

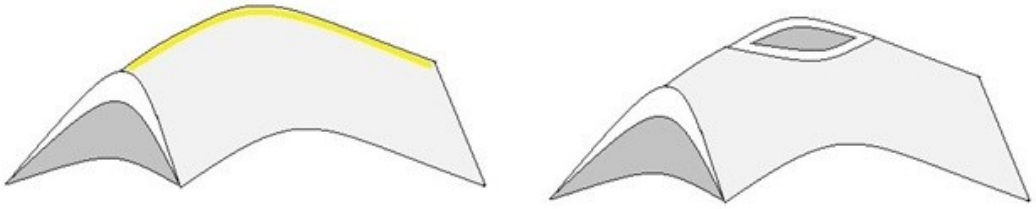

Figure 25. A non-cylindrical fold, double plunging antiform. Note the curved hinge line on top of the structure, marked with yellow.

The discontinuity of the conductivities seen in the Slingram map (Figure 24) could be a consequence of the hinge line, which is undulating between depression and culmination (Figure 26, a). The graphite is assumedly enriched in the antiforms, or in the culminations, thus causing elevated anomalies in the Slingram data. The conductive, graphite –bearing layer(s) emits an anomaly in the Slingram-map when the graphite rich fold hinge zones are located near the surface (Figure 26, b). When the conductive fold hinge zone is deeper down, the conductivity is only weakly emitted to the surface.

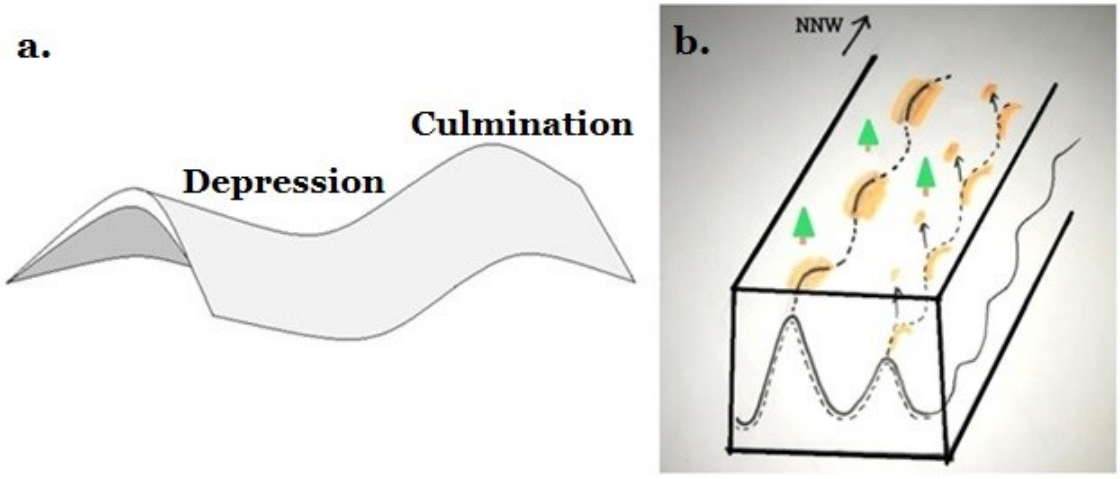

Figure 26. A) The fold hinge zone is undulating between depression and culmination. B) A schematic illustration of how the conductive graphite from the antiforms, or culminations is seen in the Slingram data. The orange color indicates elevated conductivity. When the fold hinge zones are located deeper down, the anomalies on the surface are weak. When the folds are close to the surface/ on the surface, the anomalies are stronger.

Due to graphite being mobile and working as shear strength lowering factor, it may form parasitic folds in the limbs and M-folds to the hinge zones. Similar processes have

likely been affecting both in Troms and Aitolampi, thus complicating the geometrical interpretation of the structures.

6.7 Regional structural setting

In Witicks's master's thesis (2017) a layer of garnet-bearing gneiss is present in a NW-SE-direction in Tuusniemi area, located 15 kilometers NW from Aitolampi (Figure 27). A similar garnet-bearing layer has been observed to exist in the same direction in Aitolampi area and could be interpreted as the same layer. This means that the KSdz and the garnet-bearing layer both would have the same NW-SE direction.

In the NE part of the Aitolampi study area, mylonitic structures were observed together with other signs of deformation. If the beginning of the shear zone visible in Figure 27 is drawn parallel to the garnet-bearing layer and the KSdz all the way to the mylonitic observations in Aitolampi, a structural setting in a regional scale can be constructed. The interpreted shear zone may in this thesis be called the Northern deformation zone (Ndz) in order to easier distinguish it from the KSdz. KSdz is assumed to dip towards NE and the Ndz towards SW.

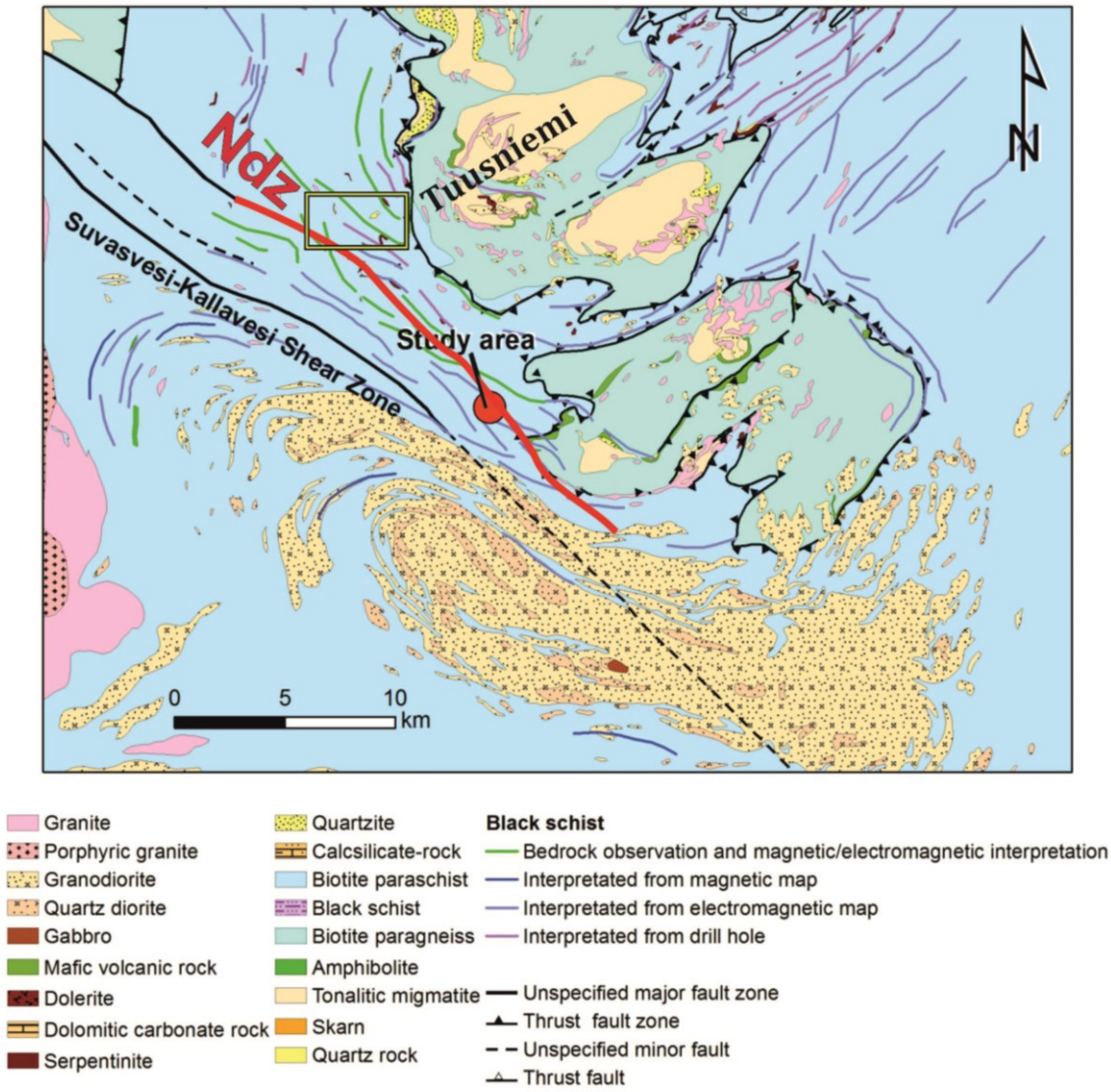

Figure 27. The Northern deformation zone (Ndz) interpreted on the bedrock map with the red line. Tuusniemi area marked with a black box. (Modified after Bedrock 1: 200 000, Geological Survey of Finland 2017)

The area has on a regional scale been subjected to several strike-slip shear systems (Sorjonen-Ward 2006). The shear systems have a NW-SE direction, which would mean a NE-SW directed compressional stress (Sorjonen-Ward 2006).

The NE-SW compressional stress squeezes the area between the shear zones and thrusts the area (block) in the middle upwards (Figure 28). This would mean that Aitolampi area would be located between two shear zones.

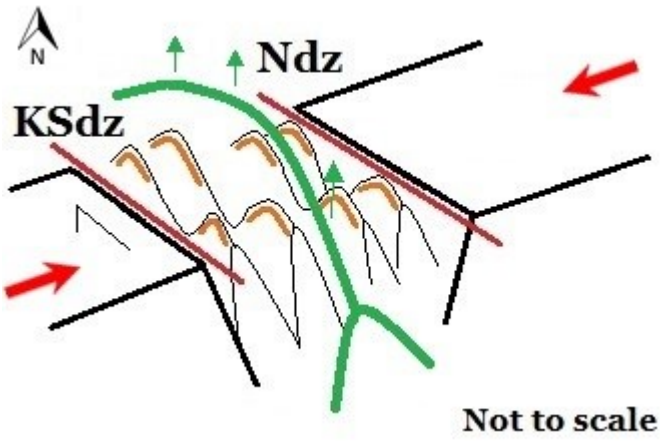

Figure 28. A schematic illustration of the study area. KSdz and Ndz are shear zones and the compressional stress (red arrows) has caused the middle part to be pushed upwards from its surroundings. The structure in the middle part is still a double plunging antiform, the green line represents the hinge line. The orange lines in the folds illustrate graphite enrichment in the antiforms.

The compressional stress may have resulted in the structures illustrated in Figure 29. Number 1 and 2 may have occurred simultaneously; reverse faulting and a strike-slip movement. These structures have resulted in number 3. The red ring marks the study area; only the Ndz can be observed in Aitolampi area. The KSdz is located some kilometers further SW from Aitolampi area and is therefore not seen in the study area.

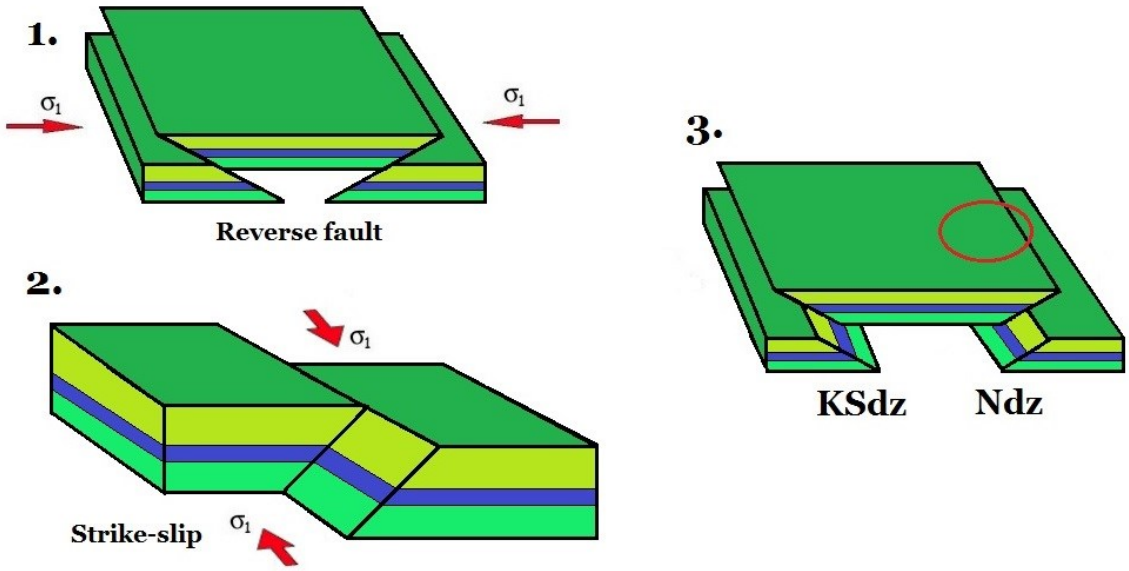

Figure 29. An illustration of the faults that could have occurred in the area, due to the presence of two shear zones. Aitolampi area marked with a red ring in illustration 3.

The shear structures seen in the middle block in the study area could be explained with Riedel-structures. Riedel structures are networks of shear bands developed in early stages of faulting. The geometry consists of conjugate shears arranged as *en-échelons* (e.g. Fossen 2011). The small-scale shearing appearing in a NW-SE direction in the middle of the study area could be an R-shear in a larger-scale Riedel structure (Figure 30). The R' structure would therefore represent a conjugate shear, visible in drill core cross cuts 1 and 7 (Figure 31). This conjugate shear would be located almost perpendicular towards KSdz. The shearing occurring in Aitolampi would therefore be shear patterns.

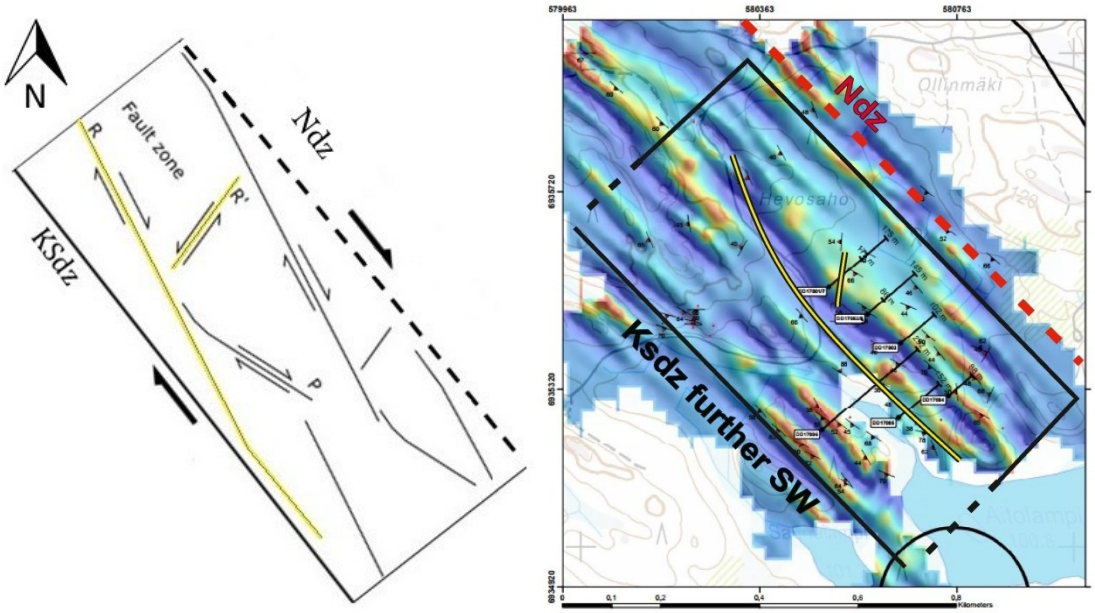

Figure 30. An illustration of a Riedel shear (left). The KSdz is the Kallavesi-Suvasvesi deformation zone, the dashed line is the interpreted Ndz, Northern deformation zone. The R and R' structures are highlighted with yellow because these structures can be observed in Aitolampi area. The right figure is showing how the Riedel structures would be plotted in Aitolampi area. The dashed lines indicate the uncertainty where the KSdz would exactly be plotted. The KSdz is most probably located some kilometers SW from the study area. (Left illustration after Fossen 2011 and right image modified after Beowulf Mining plc)

6.8. Structural cross sections of the drill holes

The data from drill core mapping and drill core cross sections was processed into a two-dimensional model, representing a sketch of the structural setting in Aitolampi study area. The Slingram-anomalies on the surface were correlated with lithologies

and elevated amounts of graphite observed from the drill cores. Some of the drill cores were drawn to the same section, due to their close location to each other (Figure 31).

The line A-B represents drillholes 1 and 7, C-D drill holes 2 and 8, E-F drill hole 3, G-H drill hole 6 and I-J drill holes 4 and 5. The 2D structural cross cuts can be seen in Appendix E.

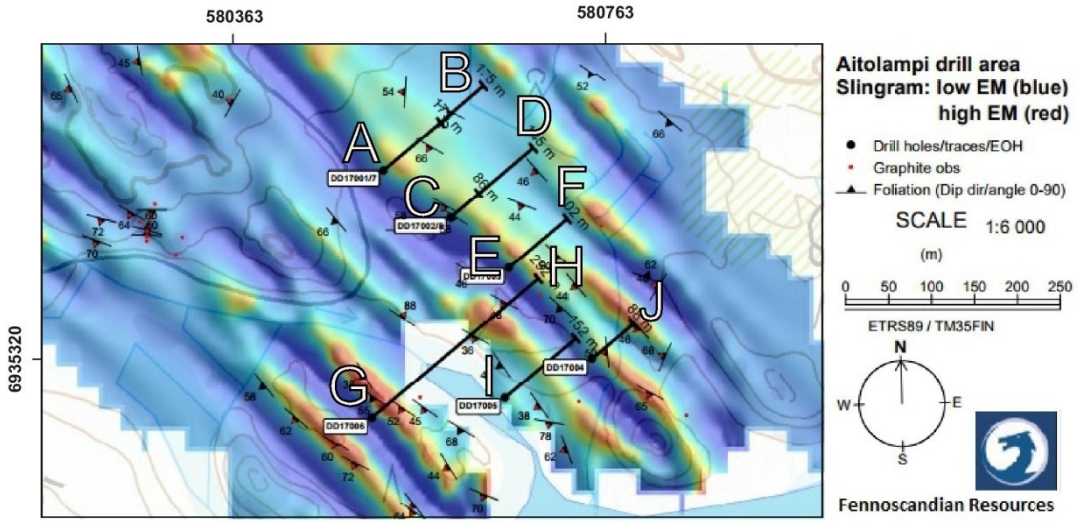

Figure 31. An illustration where the cross cuts are located in the study area. The different letters present the cross sections seen in Appendix E. (Modified after Beowulf Mining plc)

The R-shear cutting the study area in Figure 30 (right) has been interpreted in cross sections A-B, C-D, G-H and I-J as a deformation zone or strong shearing. The shear drawn perpendicular to the drill hole in cross section A-B (Figure 32) has been interpreted as a conjugate shear or as an R’ in the Riedel structures. The small parasitic folds are drawn on the fold limbs and the fold axes consist of parasitic M-folds.

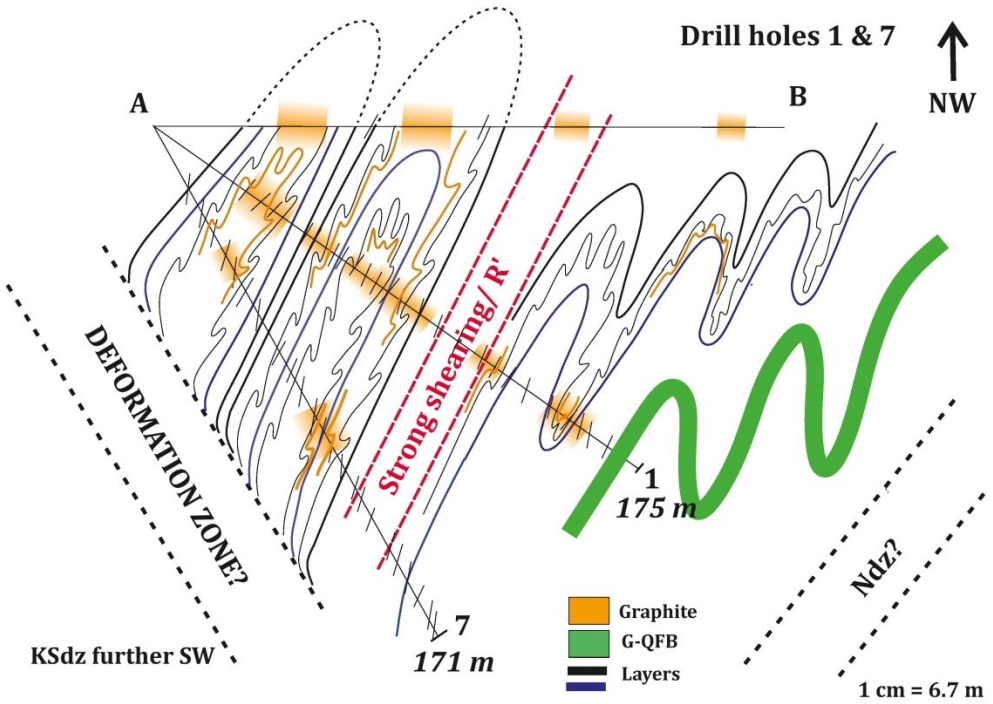

Figure 32. An illustration of cross section of A-B, drill holes 1 and 7 (see location in Figure 31). The orange color on the surface represents Slingram anomalies (elevated conductance) and in the drill cores it represents graphite, the more of the orange color the more graphite present, also in the parasitic folds. The green, curved line represents the compatible G-QFB gneiss, whose presence has made the folding more intense when the area has been affected by deformation. The parasitic folds represent the complex geometries caused by the presence of graphite. Ndz = Northern deformation zone, KSdz = Kallavesi-Suvasvesi deformation zone. The section is drawn towards NW. The scale (1 cm = 6,7 m) is not accurate anymore, since the original size of the figure had to be reduced in size. This cross cut can also be observed from Appendix E-1

6.9 Suggestions on further studies

During the field work more detailed observations of the layers with different composition could have been made. In some outcrops, layers with small variations in the grain size were noted. They could have been observed more closely, especially if there would have been differences in the foliations/ lineations or compositional variations (clay/ sandy layers) when comparing the layers.

Some fold axes would probably been easier found, if the circumstances were less snowy and the boulders better exposed.

In this thesis, the quality/type of graphite is not in main focus; during the field work some areas with flake-type graphite were observed. More concluding statements require further studies.

7. CONCLUSIONS

A structural setting in Aitolampi was built up by interpreting a combination of data from stereographic projections, drill core mapping, bedrock observations and different electromagnetic measurements. The study area is located in the middle block between two shear zones, the Kallavesi-Suvasvesi deformation zone and the Northern deformation zone. The study area is thus located in a block that has been thrusted upwards from its surroundings. A relationship between graphite-grade and structure is as follows: graphite has been enriched in fold hinge zones of antiforms in Aitolampi. The parasitic folds are present in the fold limbs, where enrichment of graphite has also occurred.

AKNOWLEDGEMENTS

I would like to thank my supervisors, Karin Högdahl (Uppsala University), Kaisa Nikkilä (Åbo Akademi University) and Sauli Raunio (Beowulf Mining plc). I would also like to thank Rasmus Blomqvist (Exploration Manager for Beowulf Mining plc) and Professor Olav Eklund (Geology and Mineralogy, ÅAU) for the magnificent opportunity to be a part of the FennoFlakes-project. I also want to thank Pietari Skyttä regarding some issues concerning structural geology. Casimir Näsi receives also a warm thank you with help regarding some it-issues and Robert Ahvonen with the much appreciated help with ArcGis (Figures 12 and 27). Sami Niemi from GTK receives a warm thank you with the Slingram advice. I am also very grateful for the help and support from Mathias Eriksson throughout the writing process. Furthermore I would like to thank everyone who has given advice, support and inspiration to write this thesis. Last but not least, I would like to thank my family and friends for the support and of course my fellow geology-students who made my time in Åbo Akademi the most wonderful and joyous.

SWEDISH SUMMARY – SVENSK SAMMANFATTNING

STRUKTURGEOLOGISK TOLKNING AV GRAFITBÄRANDE SVARTSKIFFER I AITOLAMPI, ÖSTRA FINLAND

INTRODUKTION

Grafit är ett mineral som består av tunna lager kol staplat på varandra. Ett lager av kol kallas för grafen som består av kolatomer bundna till varandra i en hexagonal tvådimensionell struktur. Grafit förekommer i tre olika former: amorft, flak- och ådergrafit (Pierson 1993).

Grafitens goda värme- och elledningsegenskaper gör den till en eftersträvad råvara inom högteknologiska tillämpningsområden (Pierson 1993). Grafit är ett av de 30 mest kritiska mineral inom EU och är till 99 % importerat (EU 2017).

Enligt Geologiska forskningscentralen i Finland (GTK) har Finland potential för nya grafitfyndigheter p.g.a. berggrundens egenskaper och en lämplig grad av metamorfos (Ahtola & Kuusela 2015).

Studieområdet Aitolampi (efter sjön Aitolampi) är beläget i Heinävesi-kommun i östra Finland, ca 50 km sydväst från staden Outokumpu. Elektromagnetiska mätningar, geologisk kartering och provtagning har gett positiva resultat gällande förekomst av grafit i Aitolampi.

Syftet med avhandlingen är att göra en strukturgeologisk tolkning över studieområdet baserat på strukturmätningar, data från borrkärnor och elektromagnetiska mätningar.

Denna pro gradu–avhandling är en del av *FennoFlakes*–projektet, i samarbete med Åbo Akademi, Geologiska Forskningscentralen i Finland och Beowulf Mining plc.

GEOLOGISK BAKGRUND

Studieområdet tillhör den Karelska provinsen inom det Nordkarelska skifferbältet. Metasedimenter som har blivit lagrade i djuphavsmiljöer och kontinentalhyllor är typiska i detta skifferbält. Kvarts-fältspat-biotit-gnejs (KFB-gnejs) är den huvudsakliga bergarten i studieområdet. Grafiten förekommer som lager och linser i svartskiffrarna inne i gnejsen.

Aitolampi är en del av det större Haapamäki-området, där grafit har blivit brutet i huvudsak på tre olika ställen främst i slutet av 1800-talet. Studieområdet kan ha en koppling till grafiten belägen i Haapamäki-vecket, men Kallavesi-Suvasvesi deformationszon (KSdz) ligger mellan studieområdet och Haapamäki-vecket, och skär därmed strukturerna.

Henderson och Kendrick (2003) har dragit slutsatsen att grafiten kan anrikas till veckomböjen och de parasitiska vecken i veckbenen. Grafiten minskar på skjuvningens motstånd och kan därmed orsaka komplexa geometrier i områden med grafit (t.ex. Oohashi 2011).

MATERIAL OCH METODER

Elektromagnetiska (EM) Slingram-mätningar har utförts i området av Beowulf Mining plc. Som en följd av grafitens höga konduktivitet, kan vissa trender observeras från Aitolampi.

Berggrundskartering utfördes för att bygga på de tidigare observationerna från Aitolampi och för att korrelera bergarterna från hällarna med observationerna från borrkärnorna.

I studieområdet borrades det totalt 1 150 meter i åtta borrhål. Borrhålen 1 och 7 samt 2 och 8 har samma startpunkt och riktning för borrning men olika stupningar. Strukturen som blev mätta från borrkärnorna projicerades till 2D-tvärsnitt.

Från varje borrhål konstruerades det en stereografisk projektion, samt en gemensam projektion från alla berggrundsobservationer med mjukvaran av R.W. Allmendinger.

RESULTAT

Från EM-data kan det observeras att de mest konduktiva områden bildar parallella ”linjer” med små diskontinuiteter i en nordvästlig-sydostlig riktning i Aitolampi.

Foliationens strykning är i medeltal 218˚ och stupning 58˚. Den huvudsakliga bergarten är KFB-gnejs. Pegmatitintrusioner med varierande riktningar observerades vid berggrundskartering.

Med hjälp av stereografiska projektioner kunde två konstruerade veckaxlar med motsatta riktningar observeras, en riktat mot nordväst och den andra mot sydost.

DISKUSSION

Det teoretiska mätningsdjupet för Slingram har en stark koppling till markens elektriska ledningsförmåga, som ställvis kan ha stora variationer (diskussion med Sami Niemi, GTK). Därmed är EM-data från Slingram riktgivande.

Vid konstruering av stereografiska projektioner lämnades vissa mätningar avsiktligen bort. Områdets storlek som blivit påverkad av frakturerna eller pegmatitintrusionerna kunde inte fastställas utifrån borrkärnorna. Detta gjordes för att erhålla så autentiska projektioner som möjligt.

En kombination av grafitens migration till lägre tryckomständigheter och gravitation kan ha lett till anrikning av grafit i antiformen. Anrikning har enligt 2D-tvärsnitt också skett i parasitvecken i veckbenen.

De två konstruerade veckaxlarna med motsatta riktningar kan tolkas som en dubbellutande antiformal struktur (*double-plunging antiform*). När veckens omböjningslinje undulerar mellan kulmination och depression kan den orsaka små diskontinuiteter synliga i EM data, om grafiten antas blivit anrikt i de antiformala

veckomböjen. Ju närmare ytan de grafitrika veckomböjen är, desto kraftigare är anomalin på ytan i Slingram-kartan.

Strukturen kan även tolkas i en regional skala. I Witick's (2017) pro gradu påstås det, att ett granatbärande lager befinner sig i nordvästlig-sydostlig riktning i Tuusniemi-området, 15 km nordväst från Aitolampi. Ett likadant lager med samma riktning kan också observeras i Aitolampi. I nordostliga delen av studieområdet har kraftig deformation med t.ex. mylonitisering observerats och kunde tolkas vara en deformationszon. Om denna skjuvzon placeras parallellt med de nordväst-sydostriktade KSdz och granatlagren, kan det påstås att Aitolampi är belägen mellan två deformationszoner. Enligt Sorjonen-Ward (2006) har området i större skala blivit utsatt för kompressional stress från nordost-sydväst. Detta kan ha gett upphov till både en revers och horisontell förkastning som resulterat i att det mittersta blocket, där Aitolampi ligger, har blivit uppskjutet från dess omgivning.

Riedel-strukturer förekommer i områden mellan två deformationszoner och består av ett nätverk av olika deformationsmönster (Fossen 2011). Riedel-strukturer i Aitolampi kan observeras både i berggrunden och i 2D tvärsnitten.

SLUTSATSER

En strukturgeologisk tolkning över studieområdet i Aitolampi konstruerades genom att kombinera data från stereografiska projektioner, borrkärnsdata, berggrundskartering och EM-data. Studieområdet finns mellan två deformationszoner och har därmed blivit upptryckt från dess omgivning. Förhållandet mellan grafithalten och strukturen i Aitolampi är följande: grafiten har anrikats i veckomböjens antiformer samt i de parasitiska vecken i veckbenen.

REFERENCES

Airo, M-L (ed.) 2005. *Aerogeophysics in Finland 1972–2004: Methods, System Characteristics and Applications.* Geological Survey of Finland, Special Paper 39. 197 pp.

Ahtola, T., Kuusela, J. 2015. *Esiselvitys Suomen grafiittipotentiaalista*. Geologian tutkimuskeskus (GTK). Report 88/2015. 14 p.

Asbury Carbons. 2016. *Graphite*. [WWW-document] *http://asbury.com/materials/graphite/* (20.10.2017)

Beowulf Mining plc. 2015-2017 in-house reports.

European Commission. 2017. *Critical raw materials*. [WWW-document] (25.1.2018)

Fossen, H. 2010. *Structural Geology* (Vol. 1): Cambridge University Press. 480 pp.

Henderson, I., Kendrick, M. 2003. *Structural controls on graphite mineralization, Senja, Troms*. Geological Survey of Norway. 110 p.

Kukkonen, I. 1984. *Grafiittipitoisten kivilajien petrofysikaaliset ominaisuudet*. Geologian tutkimuskeskus, raportti M 81/1984/4. 52 p.

Kähkönen, Y. 1998. Chapter 7 *Svekofenniset liuskealueet – merestä peruskallioksi*. In: Suomen kallioperä: 3000 vuosimiljoonaa. Helsinki, Suomen Geologinen Seura ry., pp. 199-227.

Laajoki, K. 2005. Chapter 7 *Karelian supracrustal rocks*, In: Lehtinen, M., Nurmi, P.A., Ramo, O.T. (Eds.), Precambrian Geology of Finland Key to the Evolution of the Fennoscandian Shield, Developments in Precambrian Geology. Elsevier, p. 279–341.

Laitakari, A. 1925*. Die Graphitvorkommen In Finnland und Ihre Entstehung*. Geologinen Komissioni, No. 40, 100 s.

Landis, C.A. 1971. *Graphitization of Dispersed Carbonaceous Material in Metamorphic Rocks.* Contributions to Mineralogy and Petrology, 30. pp 34-45.

Loukola-Ruskeeniemi, K. 1992. *Geochemistry of Proterozoic metamorphosed black shales in eastern Finland, with implications for exploration and environmental studies.* Academic dissertation, University of Helsinki, Department of Geology. Geological Survey of Finland, Espoo. 36 p.

Loukola-Ruskeeniemi, K., Hyvönen, E., Airo, M., Arkimaa, H., Eskelinen, J., Lerssi, J., Vanne, J., Vuoriainen, S. 2011. *Onko Suomessa uusia Talvivaara-tyyppisiä malmeja?* Geologi vol 63, pp 68- 79.

Nygård, H., 2017. *Kvalitetsbestämning av flakgrafit I Haapamäki, Leppävirta, Norra Savolax.* Master's thesis. Åbo Akademi University. 69 p.

Peltoniemi, M. 1988. *Maa- ja kallioperän geofysikaaliset tutkimusmenetelmät.* Hämeenlinna: Otakustantamo, 411 s.

Pierson, H.O. 1993. *Handbook of carbon, graphite, diamond and fullerenes - Properties, Processing and Applications*. Noyes Publications, New Jersey. 399 p.

Simandl, G.J., Paradis, S., Akam, C. 2015. *Graphite deposit types, their origin, and economic significance*. British Columbia Ministry of Energy and Mines & British Columbia Geological Survey. 2015-3, pp 163-171.

Sorjonen-Ward, P. 2006. *Geological and structural framework and preliminary interpretation of the FIRE 3 and FIRE 3A reflection seismic profiles, central Finland*. In: Kukkonen, I., Lahtinen, R. (eds.), Finnish Reflection Experiment FIRE 2001–2005, Geological Survey of Finland, Special Paper 43, 105–159.

Vuollo, J., Huhma, H. 2005. Chapter 5 *Paleoproterozoic mafic dikes in NE Finland*. , In: Lehtinen, M., Nurmi, P.A., Rämö, O.T. (Eds.), Precambrian Geology of Finland Key to the Evolution of the Fennoscandian Shield, Developments in Precambrian Geology. Elsevier, p. 195–236.

Ward, P. 1988. *Early Proterozoic Kalevian lithofacies and their interpretation in the Hammaslahti-Rääkkylä area, eastern Finland*. In: Laajoki, K., Paakkola, J. (eds.), Sedimentology of the Precambrian formations in eastern and northern Finland: Proceedings of IGCP 160 Symposium at Oulu, January 21-22, 1986, Geological Survey of Finland, Special Paper 5, 29–48.

Witick, I. 2017. *The occurrence and characterization of graphitic carbon in southern Tuusniemi, south-eastern Finland*. Sammanfattning: Förekomst och karakterisering av grafitiskt kol I södra Tuusniemi, Sydöstra Finland. Master's thesis Åbo Akademi University 52 p.

Äikäs, O. 2012. *Uraani, mustaliuske ja Talvivaara*. Geologian tutkimuskeskus (GTK). Oral presentation 22.3.2010

APPENDIX A

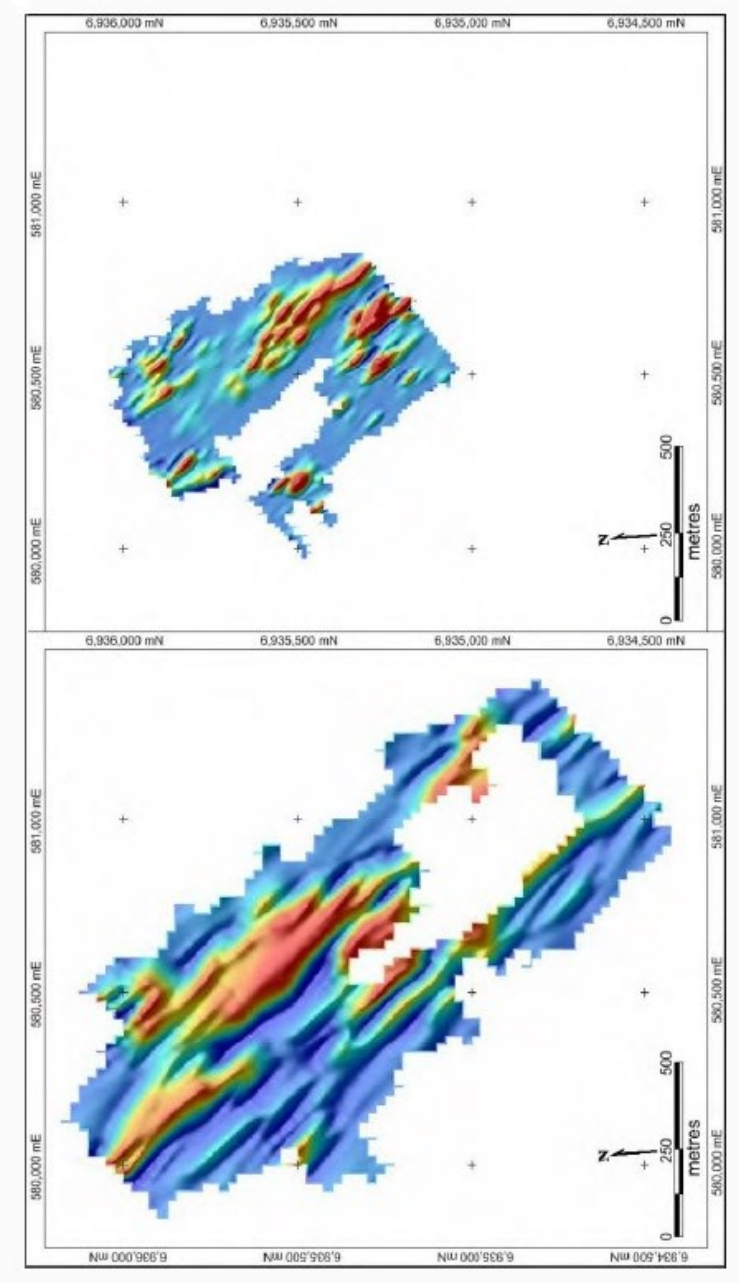

Appendix A. Comparison between Slingram (left, lower) and mini-Slingram (right, upper). It can be seen that the mini-Slingram gives smaller anomalies, whereas with the Slingram, the anomalies are broader. Both have a different penetration depth, Slingram with approximately 20 meters and mini-Slingram approximately 10 meters. Hot colors indicate areas with higher conductivity. (Beowulf Mining plc)

APPENDIX B

The coordinates are presented in the KKJ/ Zone 3, Finnish national coordinate system.

OBS_ID	EASTING	NORTHING
2016-HJN-023	3581274	6937450
2016-HJN-024	3580437	6938361
2016-HJN-025	3580507	6938661
2016-HJN-026	3580432	6938768
2016-HJN-027	3579822	6939297
2016-HJN-028	3580418	6938560
2016-HJN-029	3580527	6938514
2016-HJN-030	3580606	6938704
2016-HJN-031	3580776	6938389
2016-HJN-032	3580889	6938288
2016-HJN-033	3580934	6938163
2016-HJN-034	3580431	6938378
2016-HJN-035	3580431	6938396
2016-HJN-036	3580431	6938351
2016-HJN-037	3580692	6938165
2016-HJN-038	3580749	6938168
2016-HJN-039	3580423	6938373
2016-HJN-040	3580371	6938347
2016-HJN-041	3580472	6938355
2016-JP-024	3580365	6938763
2016-JP-025	3581059	6938147
2016-JP-026	3580672	6938791
2016-JP-027	3577855	6940577
2016-JP-028	3581304	6937135
2016-JP-029	3580211	6938904
2016-SR-023	3581185	6937540
2016-SR-024	3580540	6938652
2016-SR-025	3581037	6938487
2016-SR-026	3580133	6939280
2016-SR-027	3581088	6937617
2016-SR-028	3580272	6938834
2016-SR-029	3580960	6938368
2016-SR-030	3580431	6938370
2016-SR-031	3580431	6938384
2016-SR-032	3580431	6938356
2016-SR-033	3580602	6938140
2016-SR-034	3580648	6938111
2016-SR-035	3580752	6938152
2016-SR-036	3580339	6938526

OBS_ID	EASTING	NORTHING
2016-SR-037	3580411	6938380
2016-SR-038	3580377	6938373
2016-SR-039	3580465	6938335
2017-SR-001	3581022	6938299
2017-SR-002	3580811	6938235
2017-SR-003	3580927	6938296
2017-SR-004	3580881	6938431
2017-SR-005	3580778	6938085
2017-SR-006	3580821	6938051
2017-SR-007	3580738	6938040
2017-LP-001	3580884	6938156
2017-LP-002	3580898	6938135
2017-LP-003	3580915	6938105
2017-LP-004	3580978	6938144
2017-LP-005	3581014	6938170
2017-LP-006	3581000	6938247
2017-LP-007	3580962	6938221
2017-LP-008	3581030	6938217
2017-LP-009	3581014	6938312
2017-LP-010	3580905	6938332
2017-LP-011	3580730	6938265
2017-LP-012	3580840	6938204
2017-LP-013	3580910	6938271
2017-LP-014	3580804	6938312
2017-LP-015	3580844	6938276
2017-LP-016	3580865	6938390
2017-LP-017	3580903	6938622
2017-LP-018	3580947	6938543
2017-LP-019	3580782	6938498
2017-LP-020	3580758	6938458
2017-LP-021	3580680	6938192
2017-LP-022	3580726	6938152
2017-LP-023	3580794	6938128
2017-LP-024	3580739	6938031
2017-LP-025	3580671	6938087
2017-LP-026	3580564	6938179
2017-LP-027	3580727	6938368
2017-LP-028	3580786	6938376
2017-LP-029	3580727	6938524
2017-LP-030	3580648	6938372

APPENDIX C

The drill hole cross cuts have been constructed by Beowulf Mining plc. The red blocks on the drill holes represent the amount of graphite present as percentages. The Slingram and Mini-Slingram measurements are presented above the cross cuts. The different lithologies can also be observed from the drill cores. The structural features have not been taken into account; the lithological variations are illustrated to occur perpendicular towards the drill core. The possible curving of the drill core has been taken into account and can clearly be observed in e.g. drill hole 6 (Appendix C-3).

Appendix C-1. Cross cuts from drill holes 1 and 7, A-B. (Beowulf Mining plc)

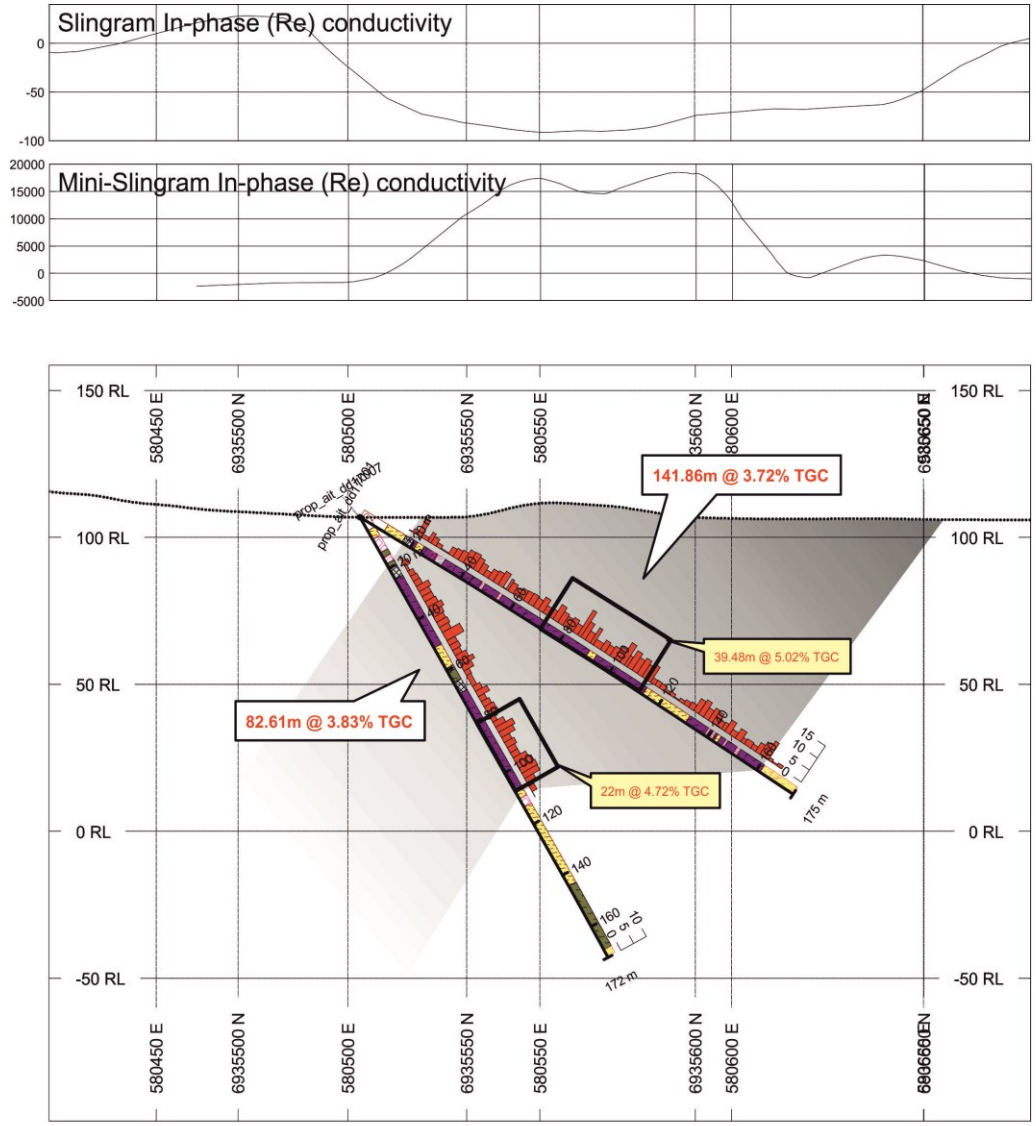

HOLES PLOTTED

TOTAL 2

prop_ait_dd17001 prop_ait_dd17007

TOPOGRAPHY

topo_line

BAR GRAPHS	L/R	COL
C-Graph_%	R	

ROCK CODES Code	PAT	LABEL	DESCRIPTION
		APL	aplite
		BX	breccia
		FZ	fault zone
		GRAF	graphite schist
		MSED	metasediment
		OVB	overburden
		PEG	pegmatite
		QFB	quartz feldspar biotite gneiss
		GQFB	garnet quartz feldspar biotite gneiss

SECTION SPECS:

REF. PT. E, N	580550 m	6935566 m
EXTENTS	334 m	257.2 m
SECTION TOP, BOT	158.6 m	-98.58 m
TOLERANCE +/-	30 m	

SCALE 1:2 000

(m)

-20 0 20 40 60 80

ETRS89 / TM35FIN

AZIMUTH = 50°

N W E S

Fennoscandian Resources

Aitolampi

6935566N SECTION

SR

Date: 18.5.2017

Appendix C-2. Cross cuts from drill holes 2 and 8, C-D. (Beowulf Mining plc)

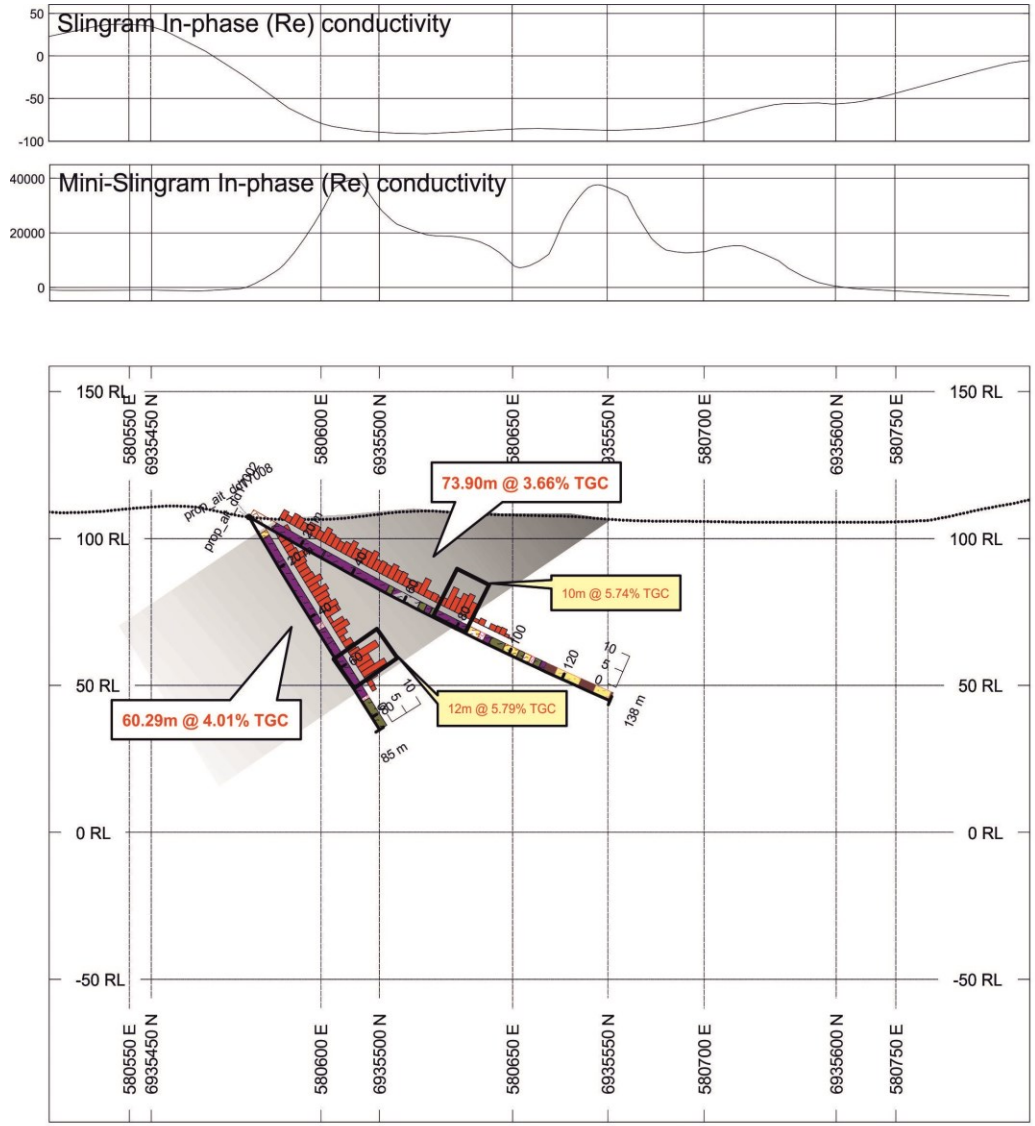

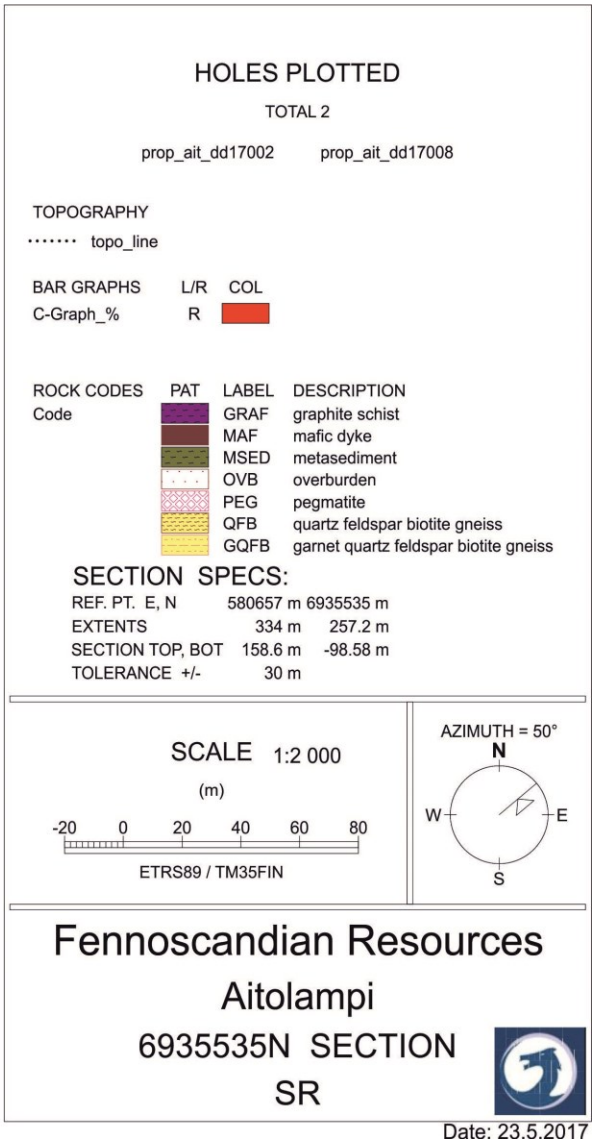

Date: 23.5.2017

Appendix C-3. Cross cuts from drill holes 3 and 6, E-F and G-H. (Beowulf Mining plc)

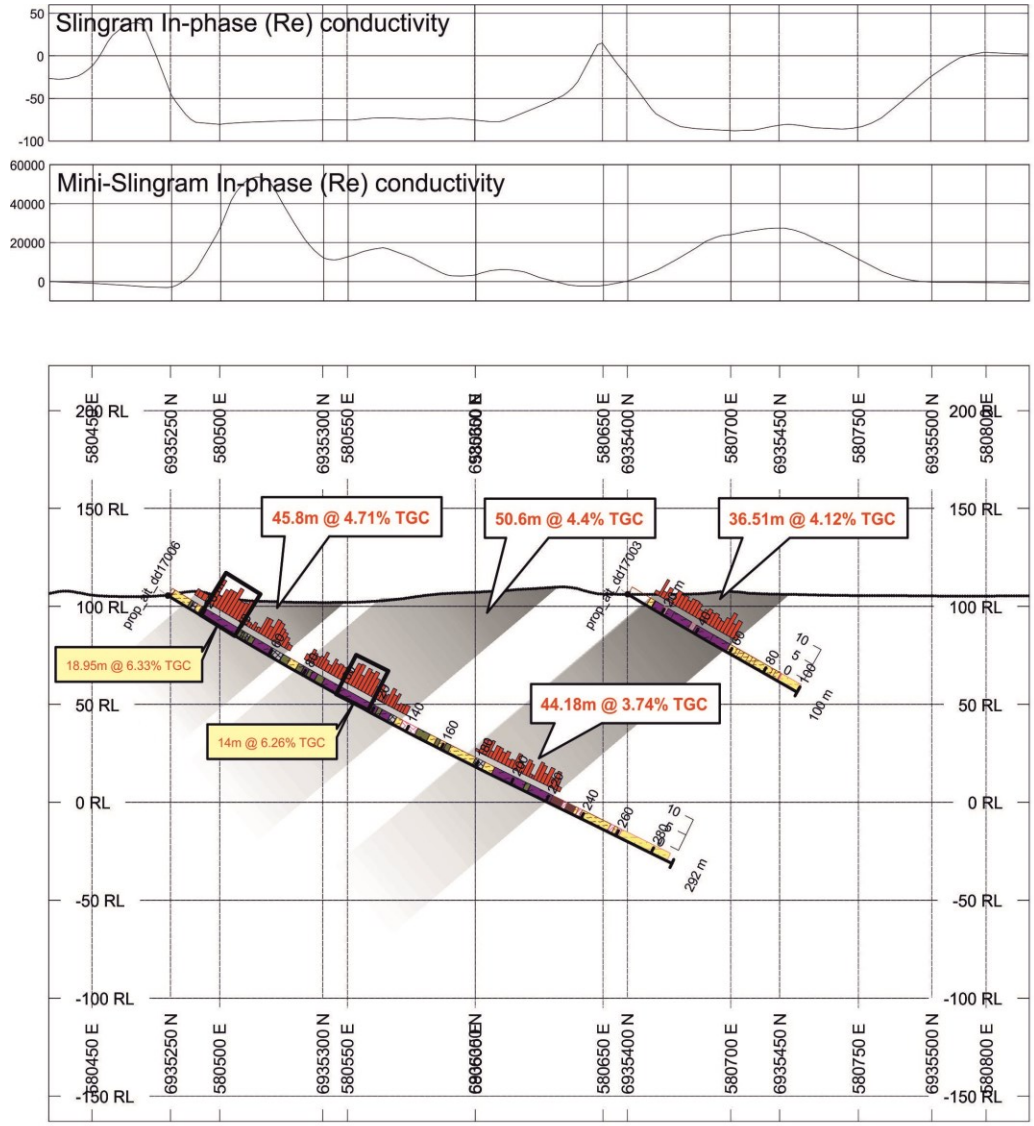

HOLES PLOTTED

TOTAL 2

prop_ait_dd17003 prop_ait_dd17006

TOPOGRAPHY

topo_line

BAR GRAPHS	L/R	COL
C-Graph_%	R	

ROCK CODES Code	PAT	LABEL	DESCRIPTION
		FZ	fault zone
		GRAF	graphite schist
		MAF	mafic dyke
		MSED	metasediment
		OVB	overburden
		PEG	pegmatite
		QFB	quartz feldspar biotite gneiss
		GQFB	garnet quartz feldspar biotite gneiss

SECTION SPECS:

REF. PT. E, N	580625 m	6935371 m
EXTENTS	501 m	385.7 m
SECTION TOP, BOT	222.9 m	-162.9 m
TOLERANCE +/-	30 m	

SCALE 1:3 000

(m)

-40 0 40 80 120

ETRS89 / TM35FIN

AZIMUTH = 50°

N W E S

Fennoscandian Resources

Aitolampi

6935371N SECTION

SR

Date: 18.5.2017

Appendix C-4. Cross cuts from drill holes 4 and 5, I-J. (Beowulf Mining plc)

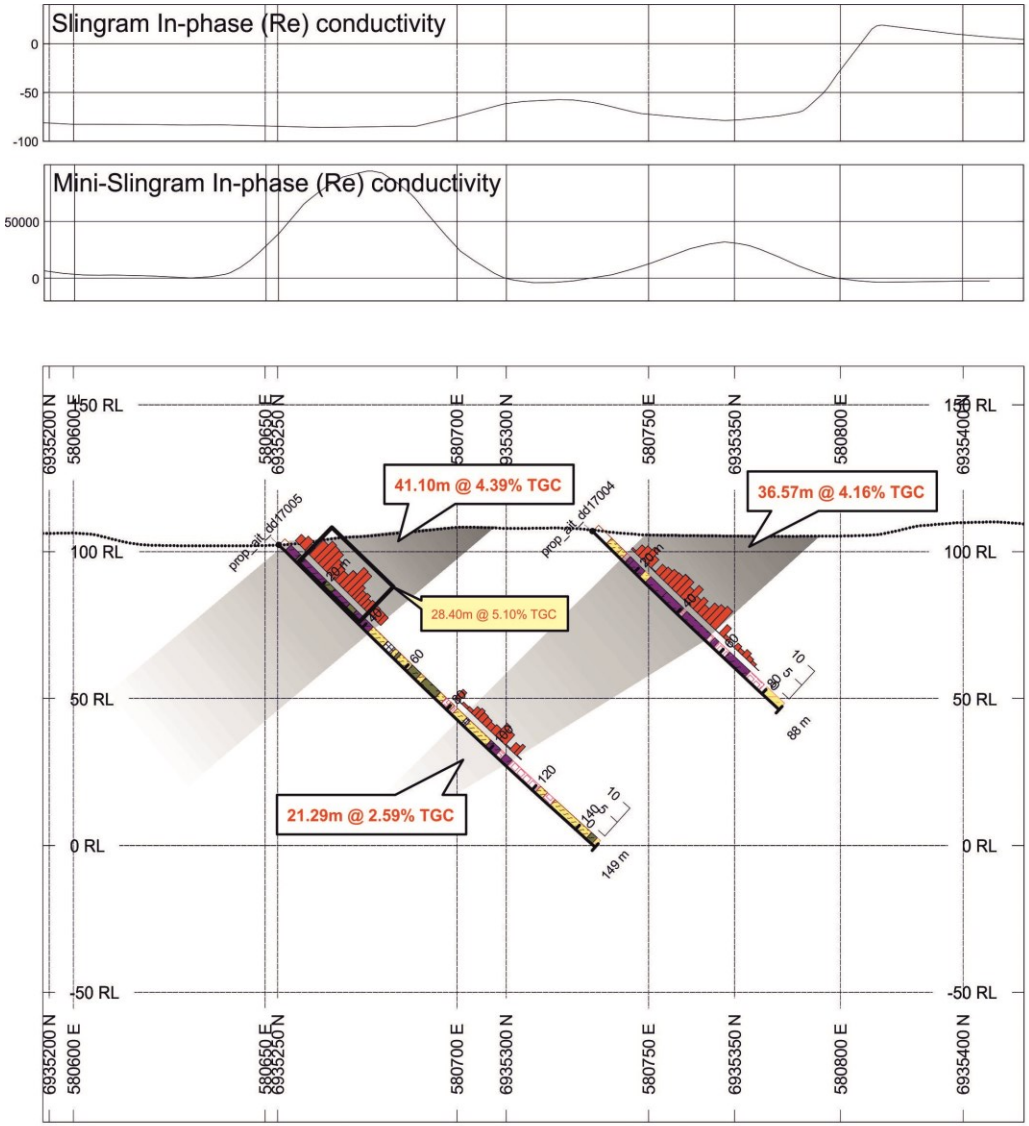

HOLES PLOTTED

TOTAL 2

prop_ait_dd17004 prop_ait_dd17005

TOPOGRAPHY

topo_line

BAR GRAPHS	L/R	COL
C-Graph_%	R	

ROCK CODES Code	PAT	LABEL	DESCRIPTION
		FZ	fault zone
		GRAF	graphite schist
		MSED	metasediment
		OVB	overburden
		PEG	pegmatite
		QF	quartz feldpar gneiss
		QFB	quartz feldspar biotite gneiss
		GQFB	garnet quartz feldspar biotite gneiss

SECTION SPECS:

REF. PT. E, N	580720 m	6935306 m
EXTENTS	334 m	257.2 m
SECTION TOP, BOT	163.1 m	-94.09 m
TOLERANCE +/-	30 m	

SCALE 1:2 000

(m)

-20 0 20 40 60 80

ETRS89 / TM35FIN

AZIMUTH = 50°

N W E S

Fennoscandian Resources

Aitolampi

6935306N SECTION

SR

Date: 23.5.2017

APPENDIX D

Collar table showing the exact locations for the drill holes.

LE ID	X (TM35FIN)	Y (TM35FIN)	Z (N2000)	DIP	AZIMUTH	EOH (m)
001	6935527.257	580500.232	106.719	-32	49	175.03
002	6935476.539	580586.902	106.337	-30	51	138.21
003	6935411.715	580648.741	105.931	-31	52	100.35
004	6935304.942	580743.664	107.069	-45	48	88.07
005	6935264.829	580647.696	102.217	-46	45	149.3
006	6935242.572	580490.623	106.000	-30	50	289.21
007	6935526.702	580499.756	106.851	-61	49	171.7
008	6935476.348	580586.655	106.300	-60	47	85.15

APPENDIX E

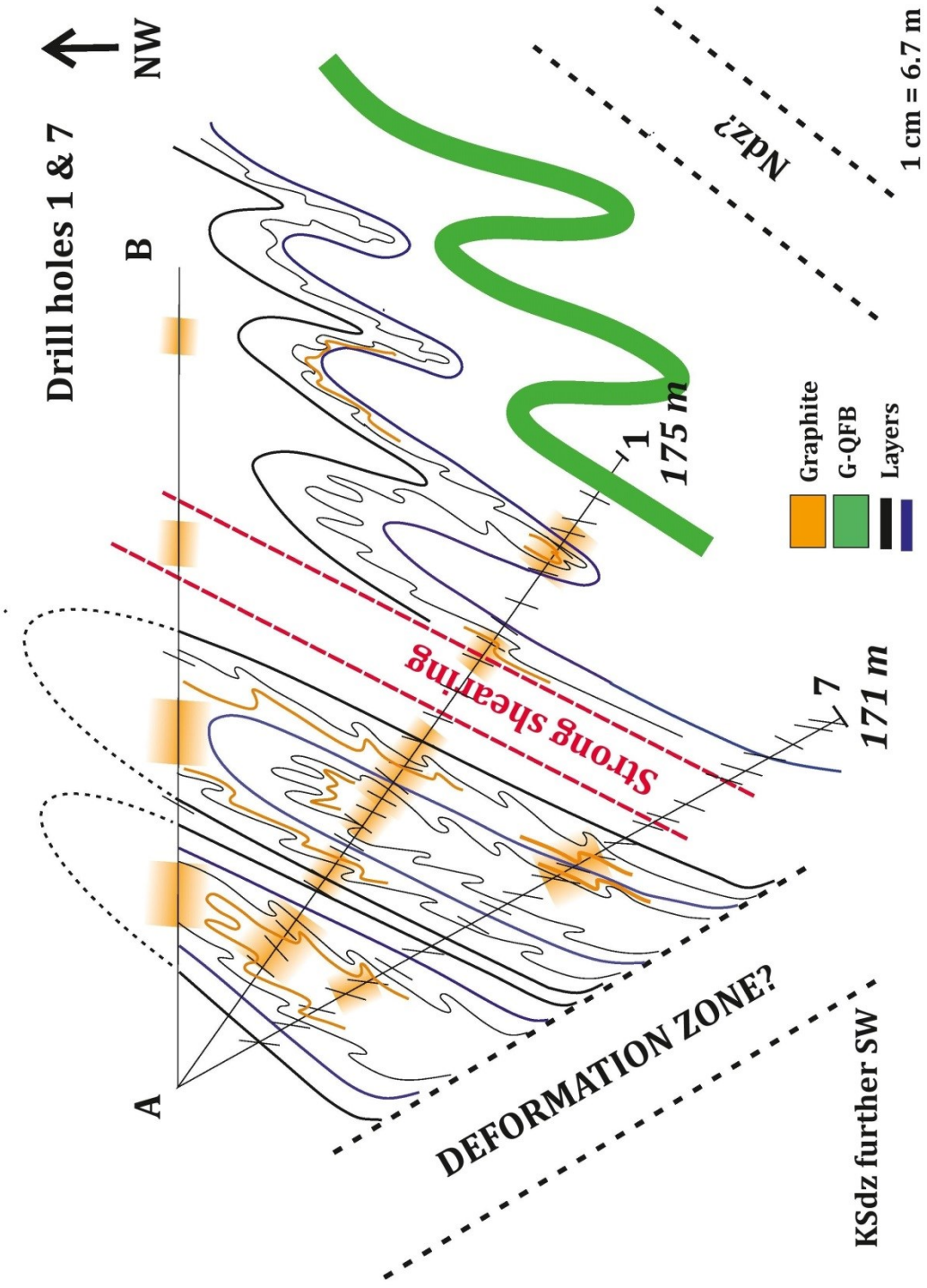

Appendix E-1. An illustration of cross section A-B, drill holes 1 and 7 (see location in Figure 31). The orange color on the surface represents Slingram anomalies (elevated conductance) and in the drill cores it represents graphite, the more of the orange color the more graphite present, also in the parasitic folds. The green, curved line represents the compatible G-QFB gneiss, whose presence has made the folding more intense when the area has been affected by deformation. The parasitic folds represent the complex geometries caused by the presence of graphite. Ndz = Northern deformation zone, KSdz = Kallavesi-Suvasvesi deformation zone. The section is drawn towards NW. The scale (1 cm = 6,7 m) is not accurate anymore, since the original size of the figure had to be reduced in size.

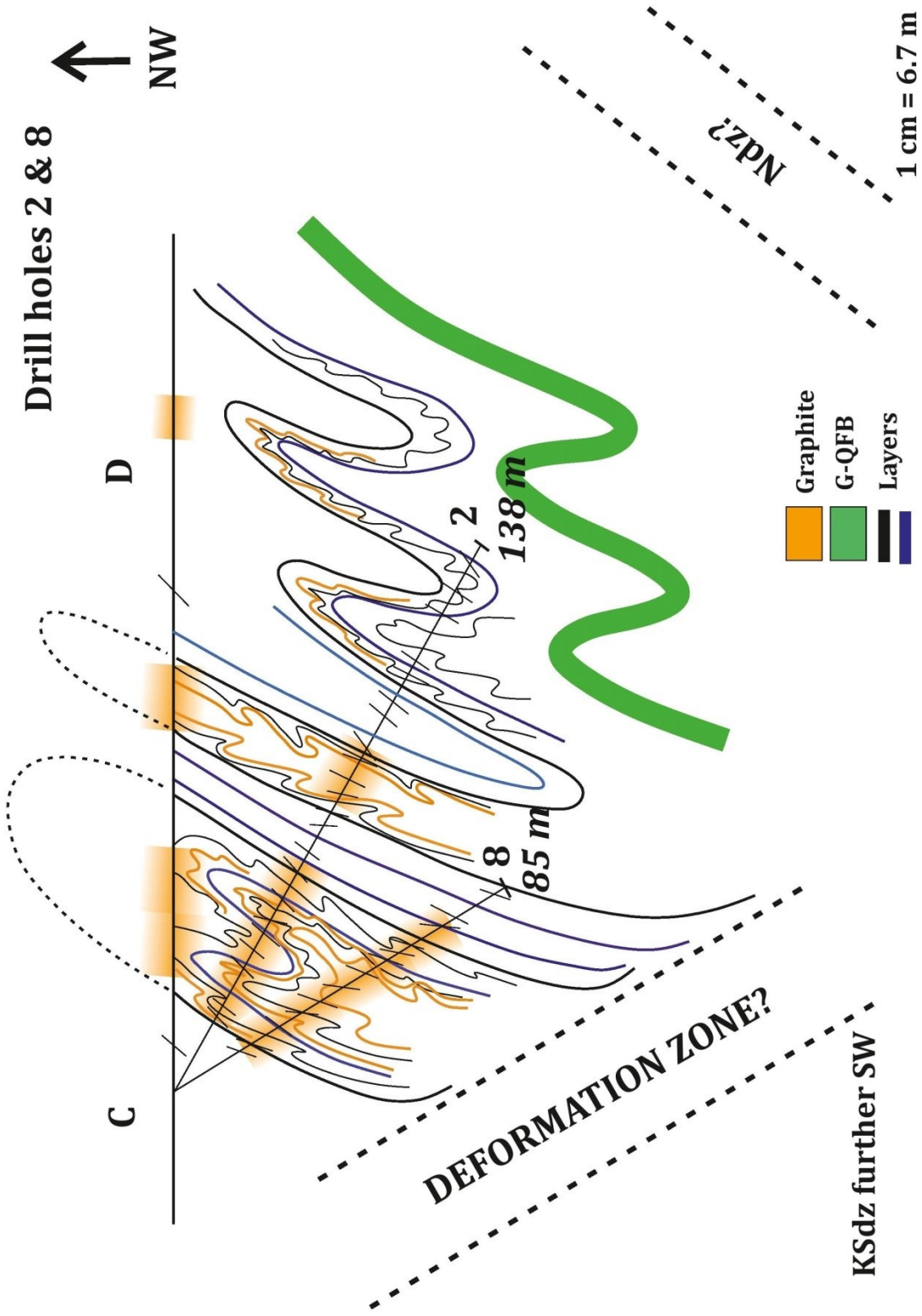

Appendix E-2. An illustration of cross section C-D, drill holes 2 and 8 (see location in Figure 31). The orange color on the surface represents Slingram anomalies (elevated conductance) and in the drill cores it represents graphite, the more of the orange color the more graphite present, also in the parasitic folds. The green, curved line represents the compatible G-QFB gneiss, whose presence has made the folding more intense when the area has been affected by deformation. The parasitic folds represent the complex geometries caused by the presence of graphite. Ndz = Northern deformation zone, KSdz = Kallavesi-Suvasvesi deformation zone. The section is drawn towards NW. The scale (1 cm = 6,7 m) is not accurate anymore, since the original size of the figure had to be reduced in size.

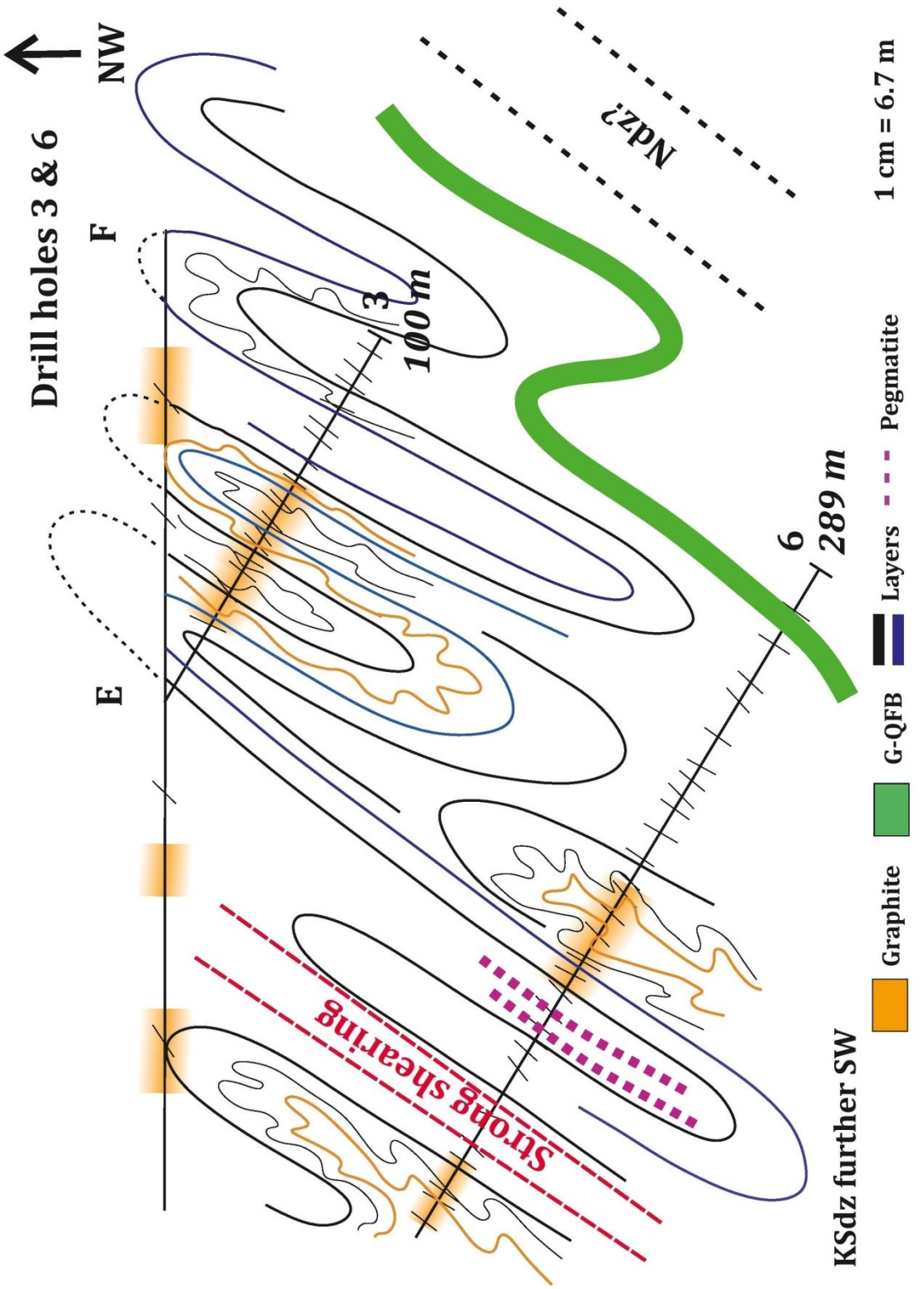

Appendix E-3. An illustration of cross section E-F, drill holes 6 and 3 (see location in Figure 31). Drill hole 6 is shown only partly, main focus on drill hole 3. The orange color on the surface represents Slingram anomalies (elevated conductance) and in the drill cores it represents graphite, the more of the orange color the more graphite present, also in the parasitic folds. The green, curved line represents the compatible G-QFB gneiss, whose presence has made the folding more intense when the area has been affected by deformation. The parasitic folds represent the complex geometries caused by the presence of graphite. Ndz = Northern deformation zone, KSdz = Kallavesi-Suvasvesi deformation zone. The section is drawn towards NW. The scale (1 cm = 6,7 m) is not accurate anymore, since the original size of the figure had to be reduced in size.

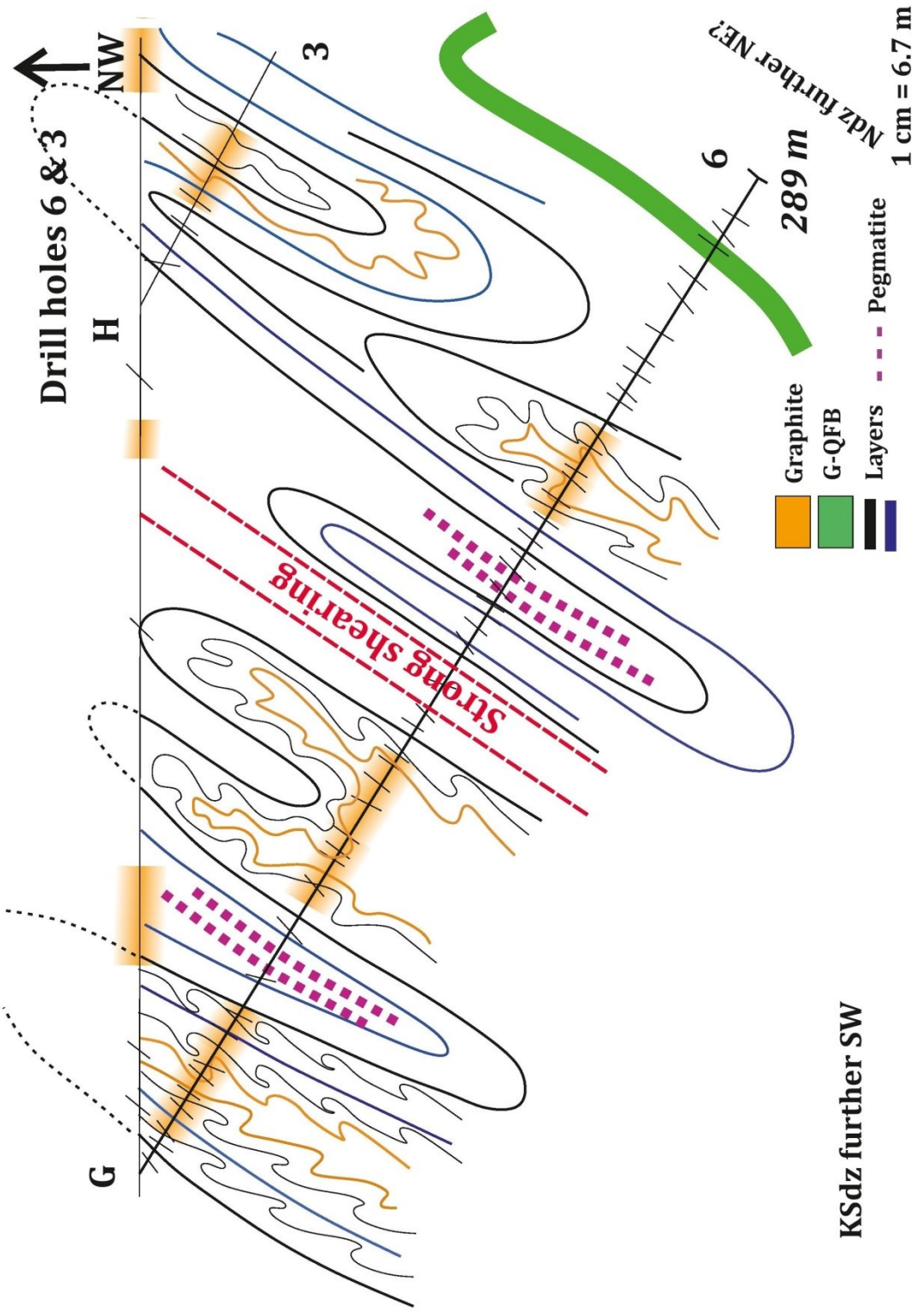

Appendix E-4. An illustration of cross section G-H, drill holes 6 and 3 (see location in Figure 31). Drill hole 3 is shown only partly, main focus on drill hole 6. The orange color on the surface represents Slingram anomalies (elevated conductance) and in the drill cores it represents graphite, the more of the orange color the more graphite present, also in the parasitic folds. The green, curved line represents the compatible G-QFB gneiss, whose presence has made the folding more intense when the area has been affected by deformation. The parasitic folds represent the complex geometries caused by the presence of graphite. Ndz = Northern deformation zone, KSdz = Kallavesi-Suvasvesi deformation zone. The section is drawn towards NW. The scale (1 cm = 6,7 m) is not accurate anymore, since the original size of the figure had to be reduced in size.

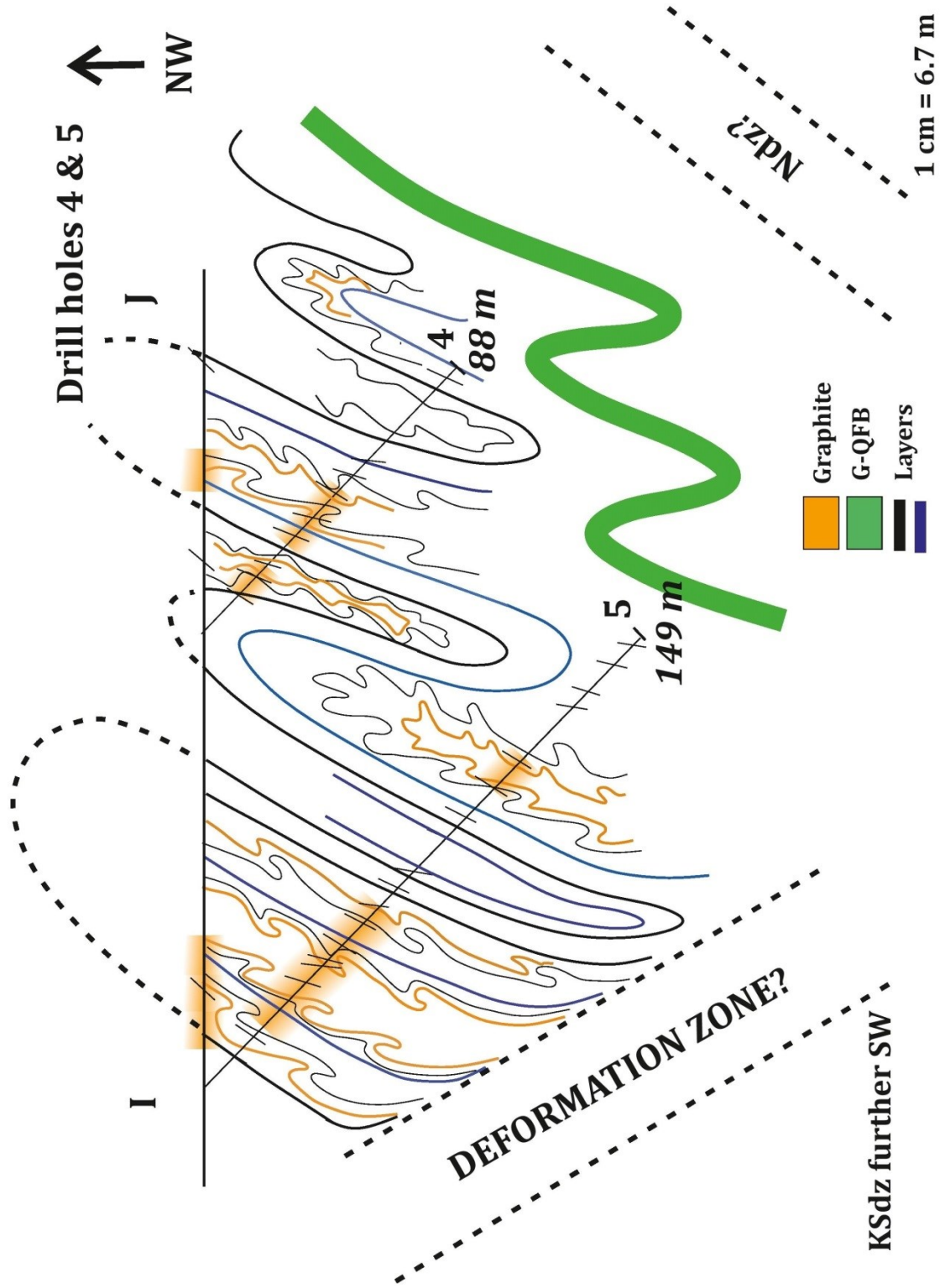

Appendix E-5. An illustration of cross section I-J, drill holes 4 and 5 (see location in Figure 31). The orange color on the surface represents Slingram anomalies (elevated conductance) and in the drill cores it represents graphite, the more of the orange color the more graphite present, also in the parasitic folds. The green, curved line represents the compatible G-QFB gneiss, whose presence has made the folding more intense when the area has been affected by deformation. The parasitic folds represent the complex geometries caused by the presence of graphite. Ndz = Northern deformation zone, KSdz = Kallavesi-Suvasvesi deformation zone. The section is drawn towards NW. The scale (1 cm = 6,7 m) is not accurate anymore, since the original size of the figure had to be reduced in size.